

Spin polaron damping in the spin-fermion model for cuprate superconductors

R.O. Kuzian

*Institute for Materials Science,
Krjijanovskogo 3,
252180 Kiev, Ukraine*

R. Hayn

*Max Planck Arbeitsgruppe Elektronensysteme,
Technische Universität Dresden,
D-01062
Dresden, Germany*

A.F. Barabanov

*Institute for High Pressure Physics,
142092 Troitsk, Moscow region, Russia*

L.A. Maksimov

*Russian Research Center Kurchatov Institute,
Kurchatov sq.46,
123182 Moscow, Russia
(April 16, 2018)*

A self-consistent, spin rotational invariant Green's function procedure has been developed to calculate the spectral function of carrier excitations in the spin-fermion model for the CuO_2 plane. We start from the mean field description of a spin polaron in the Mori-Zwanzig projection method. In order to determine the spin polaron lifetime in the self-consistent Born approximation, the self-energy is expressed by an irreducible Green's function. Both, spin polaron and bare hole spectral functions are calculated. The numerical results show a well pronounced quasiparticle peak near the bottom of the dispersion at $(\pi/2, \pi/2)$, the absence of the quasiparticle at the Γ -point, a rather large damping away from the minimum and an asymmetry of the spectral function with respect to the antiferromagnetic Brillouin zone. These findings are in qualitative agreement with photoemission data for undoped cuprates. The direct oxygen-oxygen hopping is responsible for a more isotropic minimum at $(\pi/2, \pi/2)$.

71.27.+a, 74.25.Jb, 74.72.-h

1. INTRODUCTION

In recent years there was some progress to answer the important question on the nature of quasiparticles in cuprate superconductors, but the task is not yet completed. Usually, the problem is reduced to that of the hole motion in a two dimensional quantum antiferromagnet. Many work was devoted to the t - J model¹⁻⁵ treating the antiferromagnet as a two-sublattice Néel state. It was shown that the hole motion is characterized by a quasiparticle band of bandwidth $\sim 2J$ that is separated from the incoherent part.¹⁻⁵ The minimum of the dispersion is found at the momentum $(\pi/2, \pi/2)$ (lattice constant $g = 1$) nearly degenerate with the energy at $(\pi, 0)$. Such a result was obtained by several methods. One of them is the self-consistent Born approximation (SCBA) for a reduced version of the t - J model consisting of spinless holes coupled to spinons.^{2,3,5-7} That method became especially popular since it is sufficiently simple and allows the calculation of the spectral function. It gives rise to a dispersion and also a spectral function which is symmetric with respect to the magnetic Brillouin zone (BZ). Similar results were obtained for the Emery model.⁸⁻¹⁰

In a remarkable experiment¹¹ the quasiparticle dispersion of such a spin polaron was measured directly by creating a photohole in the antiferromagnetic insulator $\text{Sr}_2\text{CuO}_2\text{Cl}_2$. Whereas the width of the

dispersion was in reasonable agreement with the theoretical predictions, its shape had some deviations especially at the point $(\pi, 0)$ in momentum space. Afterwards it was shown that the deviations can be diminished by taking into account hopping terms to second and third neighbors in the t - J model.¹²⁻¹⁴ These additional terms correspond to a proper treatment of direct oxygen-oxygen hopping in the Emery model.^{10,14} However, some deviations between theory and experiment remain. So, the measurement shows no quasiparticle weight at the Γ -point $(0, 0)$ but the spin polaron in the t - J model has. Next, one observes quite a remarkable damping especially away from the minimum. Some theories (especially the usual SCBA) are symmetric with respect to the antiferromagnetic (AFM) BZ, but the experimental data show a strong asymmetry: after crossing the AFM BZ boundary (coming from the Γ -point) the quasiparticle loses its weight nearly abruptly. That deficiency, however, seems to be merely a property of the usual SCBA and not of the t - J model itself.^{15,16}

In the usual SCBA there is no dispersion of the bare spinless hole; the dispersion appears only due to the coupling to the spinons. Therefore, one might expect large vertex corrections. In fact, however, the low order vertex corrections cancel in the pure t - J model as it was noted in Refs. 5,6. Such a cancellation is absent in the more realistic Emery model. But there are many indications (see also Ref. 17), and we will add some arguments below, that the photoemission data cannot be explained by the t - J model alone, at least not throughout the whole BZ.

We concentrate in the present paper on the spin-fermion model (the reduced form of the three-band Emery model)^{18,19} for the CuO_2 plane and present a new scheme to calculate the spectral function starting from the mean field description^{20,21} of the spin polaron. One can expect that the fluctuations around the mean field spin polaron are smaller than around the dispersionless spinless hole. The mean field description of the spin polaron in the Emery model was introduced in Refs. 20,21,26. It is based on a description of the hole motion not in the two-sublattice Néel state but in the spherically symmetric (in spin space) AFM state with long range order (LRO). Such a spin singlet state is characterized here by a vanishing expectation value of the magnetization $\langle S_i^z \rangle = 0$ (the only possible nonzero expectation values are scalars with respect to rotations in spin space), but a finite value of the spin-spin correlations at infinite distance $\langle \vec{S}_0 \vec{S}_R \rangle \rightarrow (-1)^R M$ for $R \rightarrow \infty$. It can be constructed, for instance, from a resonating valence bond (RVB) state with long-range bonds that decay not too fast.²² The spherically symmetric state is an appealing candidate to study the transition from the paramagnetic spin liquid (with only short range correlations) to a state with long-range order.

A spherically symmetric Green's function (GF) theory for Heisenberg models was constructed by Kondo and Yamaji (KY)²³ and it will be used as one ingredient of the present theory. It is a GF decoupling scheme which is applicable to cases in which there is no symmetry breaking, especially to low dimensional systems (for the 2D square lattice see Refs. 24,25). As a result, the carrier excitations (moving in the spherically symmetric background) preserve the periodicity relative to the full BZ (not the magnetic one). Namely this leads to a qualitative agreement with the experimental results in the undoped compound $\text{Sr}_2\text{CuO}_2\text{Cl}_2$. An explanation might be that the actual experiment was done at room temperature, whereas the Néel temperature of $\text{Sr}_2\text{CuO}_2\text{Cl}_2$ is only 250 K.

The aim of the present work is twofold. In the first place it is a methodical work proposing a new technique to calculate the spectral function of quasiparticles with complicated operator structure. Our technique combines the Mori-Zwanzig projection method with a self-consistent calculation of the self-energy in terms of irreducible GF (Tserkovnikov technique²⁷). In difference to our recent works^{28,29} we introduce a simultaneous description of a spin polaron and a bare hole, and investigate the effects of direct oxygen-oxygen hopping which only gives us the possibility to reach a realistic description. Furthermore, we discuss also the upper parts of the spectrum in the spin-fermion model whose lowest branch corresponds to the spin polaron. The second aim is to present numerical results for the spectral function. We will distinguish three regions in \mathbf{k} -space where the spin polaron exists as a quasiparticle with infinite lifetime, with finite lifetime or where it is strongly overdamped. Our method leads to several, qualitatively new features which are not present in the SCBA of spinless holes coupled to spinons. But these features may be observed in the experimental data for $\text{Sr}_2\text{CuO}_2\text{Cl}_2$. We are concentrating here on a qualitative discussion rather than fine tuning the parameters of the Emery model in its spin-fermion form to obtain maximal agreement with experiment.

Our paper is organized as follows: after presenting the set of basis operators which define the mean

field description of the spin polaron (Sec. 3) we show the general procedure to calculate the damping (Sec. 4) and calculate the corresponding vertex (Sec. 5). The self-consistent set of equations for the GF is given in Sec. 6 and the results are presented in Sec. 7.

2. SPIN-FERMION MODEL

An extra hole propagating in the CuO₂ plane of cuprates strongly interacts with the antiferromagnetically correlated copper spin subsystem. The main features of the hole motion are described by the model:^{18,19}

$$\hat{H} = \hat{\tau} + \hat{J} + \hat{h}, \quad (2.1)$$

$$\hat{\tau} = 4\tau \sum_{\mathbf{R}} p_{\mathbf{R}}^{\dagger} \left(\frac{1}{2} + \tilde{S}_{\mathbf{R}} \right) p_{\mathbf{R}}, \quad \hat{J} = \frac{J}{2} \sum_{\mathbf{R}, \mathbf{g}} S_{\mathbf{R}}^{\alpha} S_{\mathbf{R}+\mathbf{g}}^{\alpha}, \quad (2.2)$$

$$\hat{h} = -h \sum_{\mathbf{R}} \left[c_{\mathbf{R}+\mathbf{a}_x}^{\dagger} (c_{\mathbf{R}+\mathbf{a}_y} + c_{\mathbf{R}-\mathbf{a}_y} + c_{\mathbf{R}+\mathbf{g}_x+\mathbf{a}_y} + c_{\mathbf{R}+\mathbf{g}_x-\mathbf{a}_y}) + h.c. \right], \quad (2.3)$$

with

$$p_{\mathbf{R}} = \frac{1}{2} \sum_{\mathbf{a}} c_{\mathbf{R}+\mathbf{a}}, \quad \tilde{S}_{\mathbf{R}} \equiv S_{\mathbf{R}}^{\alpha} \hat{\sigma}^{\alpha}, \quad \{p_{\mathbf{R}}, p_{\mathbf{R}'}^{\dagger}\} = \delta_{\mathbf{R}, \mathbf{R}'} + \frac{1}{4} \sum_{\mathbf{g}} \delta_{\mathbf{R}, \mathbf{R}'+\mathbf{g}}, \quad (2.4)$$

where $\mathbf{a}_{x,y} = \frac{1}{2}\mathbf{g}_{x,y}$, $\mathbf{g} = \pm\mathbf{g}_x, \pm\mathbf{g}_y$.

Here and below the summation over repeated indexes is understood everywhere; $\{\dots, \dots\}$, $[\dots, \dots]$ stand for anticommutator and commutator respectively; $\mathbf{g}_{x,y}$ are basis vectors of a copper square lattice ($|\mathbf{g}| \equiv 1$), $\mathbf{R} + \mathbf{a}$ are four vectors of O sites nearest to the Cu site \mathbf{R} ; the operator $c_{\mathbf{R}+\mathbf{a}}^{\dagger}$ creates a hole predominantly at the O site (the spin index is dropped in order to simplify the notations); $\hat{\sigma}^{\alpha}$ are the Pauli matrices; the operator \mathbf{S} represents the localized spin on the copper site. We do not introduce the explicit relative phases of p - and d -orbitals since they can be transformed out by redefining the operators with phase factors $\exp(i\mathbf{q}_0 \cdot \mathbf{R})$, $\mathbf{q}_0 = (\pi, \pi)$. In order to compare our results with other authors and with experiment we restore these phases by changing in the final results $\mathbf{k} \rightarrow \mathbf{k}' = \mathbf{k} - \mathbf{q}_0$. The parameter τ is the hopping amplitude of oxygen holes that take into account the coupling of the hole motion with the copper spin subsystem, J is the constant of nearest neighbor AFM exchange between the copper spins. For the parameter values we take $\tau \sim 0.5\text{eV}$, $J = 0.2\tau$ throughout the paper, $h = 0$, or $h = 0.3\tau$ to illustrate the influence of direct oxygen-oxygen hopping.

The Hamiltonian (2.1) corresponds to the regime $U_d \gg |\varepsilon_p - \varepsilon_d| \gg t_{pd}$ in the Emery model. It can be obtained³⁰ e.g. by a canonical transformation of bare fermion operators $\bar{a} = e^{-S} a e^S$. Then the transformed operators a which enter the Hamiltonian (2.1) acquire the admixture of bare operators at adjacent sites. For example, the "oxygen hole" operator in the Eq. (2.3) may be expressed as

$$c_{\mathbf{R}+\mathbf{a},s} = e^{\bar{S}} \bar{c}_{\mathbf{R}+\mathbf{a},s} e^{-\bar{S}} \approx \bar{c}_{\mathbf{R}+\mathbf{a},s} + \frac{t_{pd}}{|\varepsilon_p - \varepsilon_d|} \bar{d}_{\mathbf{R},s} \left(1 - \bar{d}_{\mathbf{R},-s}^{\dagger} \bar{d}_{\mathbf{R},-s} \right). \quad (2.5)$$

This operator annihilates the hole in a state that is an antibonding (in hole notation) combination of the oxygen p_{σ} state and the singly occupied copper $d_{x^2-y^2}$ state at adjacent sites.

The non-bosonic character of spin operators and the complexity of the spin subsystem ground state $|\mathcal{G}\rangle$ make a perturbative treatment of the Hamiltonian (2.1) difficult. For this reason we develop in the next sections the method of Green's function calculation which combine the Mori-Zwanzig projection method (PM)^{31,32} with the Tserkovnikov technique. The PM provides the possibility to allow for the local correlations thoroughly. For example, the local constraints are naturally included in the calculation. We thus obtain the proper description of small polaron (so called Zhang-Rice (ZR) singlet)^{20,33} formation

that is governed by the Kondo term in $\hat{\tau}$. On the other hand, the PM always provides the Green's function as the sum of simple poles, since only a finite number of basis operators may be included in the calculation. The consideration of polaron scattering on spin excitations, which is responsible for the damping of the polaron state, demands an infinite extension of the basis set. This can be done effectively by the self-consistent Born approximation (SCBA) for the polaron self-energy, calculated within the Tserkovnikov technique.²⁷ That means that we suppose the effect of the residual polaron-spin interaction to be rather small and tractable within a self-consistent perturbative scheme. The main point here is the appropriate choice of the operator basis set for PM and a careful division of the interaction into mean field and residual part.

3. BASIS OPERATORS AND PROJECTION METHOD

From the very beginning we want to take into account properly the local correlations $\hat{\tau}$ without the violation of spin commutation relations. We consider a spin-liquid state with spin rotational symmetry for the copper subsystem, e.g. the spin-spin correlation functions satisfy the relation $C_{\mathbf{r}} \equiv \langle S_{\mathbf{R}}^{\alpha} S_{\mathbf{R}+\mathbf{r}}^{\alpha} \rangle = 3 \langle S_{\mathbf{R}}^{x(y,z)} S_{\mathbf{R}+\mathbf{r}}^{x(y,z)} \rangle$. We choose a set of three basis operators. The first two of them constitute the ZR polaron

$$B_{1,\mathbf{k}} = \frac{1}{\beta_{\mathbf{k}} \sqrt{N}} \sum_{\mathbf{R}} e^{-i\mathbf{k}\mathbf{R}} p_{\mathbf{R}}, \quad B_{2,\mathbf{k}} = \frac{1}{\nu_{\mathbf{k}} \sqrt{N}} \sum_{\mathbf{R}} e^{-i\mathbf{k}\mathbf{R}} \tilde{S}_{\mathbf{R}} p_{\mathbf{R}}, \quad (3.1)$$

where the factors $\beta_{\mathbf{k}}$ and $\nu_{\mathbf{k}}$ arise due to the orthonormalization

$$\beta_{\mathbf{k}} = \sqrt{1 + \gamma_{\mathbf{k}}}, \quad \nu_{\mathbf{k}} = \sqrt{\frac{3}{4} + C_{\mathbf{g}} \gamma_{\mathbf{k}}}, \quad (3.2)$$

and $\gamma_{\mathbf{k}} \equiv \frac{1}{2} (\cos k_x + \cos k_y)$. In fact, the basis operators (3.1) can be combined in two ways corresponding to the ZR singlet and part of the ZR triplet state. Only the lower lying singlet combination builds the spin polaron quasiparticle. We can also write

$$B_{1,\mathbf{k}} = \frac{1}{\beta_{\mathbf{k}}} \left[\cos\left(\frac{k_x}{2}\right) c_{\mathbf{k},x} + \cos\left(\frac{k_y}{2}\right) c_{\mathbf{k},y} \right] \quad (3.3)$$

where

$$c_{\mathbf{k},x,y} = \frac{1}{\sqrt{N}} \sum_{\mathbf{R}} e^{-i\mathbf{k}(\mathbf{R}+\mathbf{a}_{x,y})} c_{\mathbf{R}+\mathbf{a}_{x,y}}.$$

Now it is easy to see that one has to introduce the operator

$$B_{3,\mathbf{k}} = \frac{1}{\beta_{\mathbf{k}}} \left[\cos\left(\frac{k_y}{2}\right) c_{\mathbf{k},x} - \cos\left(\frac{k_x}{2}\right) c_{\mathbf{k},y} \right] \quad (3.4)$$

in order to represent the full set of bare hole operators. That is important if we want to find the hole spectral weight of the spin polaron band.

In a first step we construct the three eigenoperators $\mathcal{B}_{i,\mathbf{k}}$ and the corresponding bands $\Omega_{\mathbf{k}}^{(i)}$ in the mean field approach:

$$\mathcal{B}_{i,\mathbf{k}} = \alpha_j^{(i)}(\mathbf{k}) B_{j,\mathbf{k}}, \quad \mathcal{B}_{\mathbf{k}} \equiv \mathcal{B}_{1,\mathbf{k}}, \quad \Omega_{\mathbf{k}} \equiv \Omega_{\mathbf{k}}^{(1)}, \quad (3.5)$$

where we introduced a simplified notation for the most interesting lowest spin polaron band $\Omega_{\mathbf{k}}$ with the polaron annihilation eigenoperator $\mathcal{B}_{\mathbf{k}}$. We use the projection method of Mori and Zwanzig^{31,32} and introduce the retarded Green's functions (GF):

$$G_{ij}(\mathbf{k}, \omega) = \langle B_{i,\mathbf{k}} | B_{j,\mathbf{k}}^\dagger \rangle_\omega \equiv -i \int_{t'}^\infty dt e^{i\omega(t-t')} \langle \{ B_{i,\mathbf{k}}(t), B_{j,\mathbf{k}}^\dagger(t') \} \rangle. \quad (3.6)$$

Here we use Zubarev's notations.³⁴ Within the PM the equations of motion for the GF (3.6) are projected onto the subspace spanned by the operators $B_{i,\mathbf{k}}$ which leads to the following eigenvalue problem to determine $\alpha_j^{(n)}$ and $\Omega_{\mathbf{k}}^{(n)}$:

$$\omega G_{ij}^{(0)}(\mathbf{k}, \omega) = \delta_{ij} + \mathcal{L}_{il} G_{lj}^{(0)}(\mathbf{k}, \omega), \quad \left(\mathcal{L}_{ij} - \Omega_{\mathbf{k}}^{(n)} \delta_{ij} \right) \alpha_j^{(n)}(\mathbf{k}) = 0 \quad (3.7)$$

where

$$\mathcal{L}_{ij} \equiv \left\langle \left\{ \left[B_{i,\mathbf{k}}, \hat{H} \right], B_{j,\mathbf{k}}^\dagger \right\} \right\rangle; \quad \left\langle \left\{ B_{i,\mathbf{k}}, B_{j,\mathbf{k}}^\dagger \right\} \right\rangle = \delta_{ij}. \quad (3.8)$$

An explicit calculation expresses \mathcal{L}_{ij} in terms of the two-site spin-spin correlation functions $C_{\mathbf{r}}$ and gives:

$$\begin{aligned} \mathcal{L}_{11} &= 2\tau\beta_{\mathbf{k}}^2 - \frac{8h\pi_{\mathbf{k}}^2}{\beta_{\mathbf{k}}^2}, \quad \mathcal{L}_{12} = \mathcal{L}_{21} = 4\tau\beta_{\mathbf{k}}\nu_{\mathbf{k}}, \quad \mathcal{L}_{13} = \mathcal{L}_{31} = -\frac{4h\pi_{\mathbf{k}}\delta_{\mathbf{k}}}{\beta_{\mathbf{k}}^2}, \\ \mathcal{L}_{22} &= \frac{\tau}{\nu_{\mathbf{k}}^2} \left[-\frac{9}{8} + C_{\mathbf{g}}(1 - 4\gamma_{\mathbf{k}}) + \frac{1}{8} \sum_{\mathbf{g}_1 \neq \mathbf{g}_2} e^{-i\mathbf{k}(\mathbf{g}_1 - \mathbf{g}_2)} C_{\mathbf{g}_1 - \mathbf{g}_2} \right] \\ &\quad + \frac{J}{\nu_{\mathbf{k}}^2} C_{\mathbf{g}}(\gamma_{\mathbf{k}} - 4) - \frac{h}{\nu_{\mathbf{k}}^2} \left[\frac{3}{2} + 4C_{\mathbf{g}}\gamma_{\mathbf{k}} + 2C_{\mathbf{g}_x + \mathbf{g}_y}(\gamma_{\mathbf{k}}^2 - \delta_{\mathbf{k}}^2) \right], \\ \mathcal{L}_{23} = \mathcal{L}_{32} &= 0, \quad \mathcal{L}_{33} = \frac{8h\pi_{\mathbf{k}}^2}{\beta_{\mathbf{k}}^2} \end{aligned} \quad (3.9)$$

where

$$\delta_{\mathbf{k}} \equiv \frac{1}{2}(-\cos k_x + \cos k_y), \quad \pi_{\mathbf{k}} \equiv \cos\left(\frac{k_x}{2}\right) \cos\left(\frac{k_y}{2}\right).$$

The projected equation of motion (3.7) defines the mean field Green's functions $G_{ij}^{(0)}$ with three bands $\Omega_{\mathbf{k}} = \Omega_{\mathbf{k}}^{(1)}, \dots, \Omega_{\mathbf{k}}^{(3)}$ corresponding to the ZR singlet, the nonbonding oxygen and the triplet bands. The mean field spectrum of all three bands is shown in Figs. 1(a) and 1(b) for two different parameter sets. In the following we will mainly concentrate on the eigenoperator of the lowest band, the polaron eigenoperator $\mathcal{B}_{\mathbf{k}} = \mathcal{B}_{1,\mathbf{k}}$. The GF of the polaron quasiparticle is defined as:

$$G_p(\mathbf{k}, \omega) = \langle \mathcal{B}_{\mathbf{k}} | \mathcal{B}_{\mathbf{k}}^\dagger \rangle_\omega. \quad (3.10)$$

One has to distinguish between the polaron GF defined in (3.10) and the GF $G_h(\mathbf{k}, \omega)$ which gives the number of holes in a unit cell and is introduced as:

$$G_h(\mathbf{k}, \omega) = \langle c_{\mathbf{k},x} | c_{\mathbf{k},x}^\dagger \rangle_\omega + \langle c_{\mathbf{k},y} | c_{\mathbf{k},y}^\dagger \rangle_\omega = \langle B_{1,\mathbf{k}} | B_{1,\mathbf{k}}^\dagger \rangle_\omega + \langle B_{3,\mathbf{k}} | B_{3,\mathbf{k}}^\dagger \rangle_\omega. \quad (3.11)$$

Please note that according to (2.5) the GF G_h counts not only the holes at oxygen sites, but has a contribution at the copper sites also. Below we shall suppose that the intensity given by the photoemission experiments can be roughly compared with the hole spectral function which is dictated by $G_h(\mathbf{k}, \omega)$. In the mean field approximation $G_h^{(0)}(\mathbf{k}, \omega)$ has the form

$$G_h^{(0)}(\mathbf{k}, \omega) = \sum_i \frac{|\alpha_1^{(i)}(\mathbf{k})|^2 + |\alpha_3^{(i)}(\mathbf{k})|^2}{\omega - \Omega_{\mathbf{k}}^{(i)}} = \sum_i \frac{Z^{(i)}(\mathbf{k})}{\omega - \Omega_{\mathbf{k}}^{(i)}}, \quad (3.12)$$

which defines the pole strength $Z^{(i)}(\mathbf{k})$ of all three bands. If we restrict ourselves to the vicinity of the lowest pole $\Omega_{\mathbf{k}} = \Omega_{\mathbf{k}}^{(1)}$ the hole GF can be approximated by

$$G_h^{(0)}(\mathbf{k}, \omega) \approx Z(\mathbf{k})G_p^{(0)}(\mathbf{k}, \omega), \quad (3.13)$$

with

$$Z(\mathbf{k}) = Z^{(1)}(\mathbf{k}), \quad \text{and} \quad G_p^{(0)} = \frac{1}{\omega - \Omega_{\mathbf{k}}}. \quad (3.14)$$

Let us first discuss the mean field spectrum of all three bands for the two parameter sets with and without direct oxygen-oxygen hopping h (Figs. 1(a) and 1(b)). First of all, one observes a well separated singlet band between 1 and 2 eV below the nonbonding one. The singlet-triplet splitting is maximal at (π, π) and roughly 3 eV (assuming τ to be 0.5 eV). That agrees quite reasonably with the splitting between the ZR singlet and triplet states of 3.4 eV that were found in calculations for a CuO_4 cluster.³⁵ And experimental indications for the triplet state were found in a recent photoemission measurement of the substance $\text{Ba}_2\text{Cu}_3\text{O}_4\text{Cl}_2$.³⁶ It is also interesting to note that the singlet band dispersion obeys nearly the antiferromagnetic symmetry (with only small deviations due to the spin rotational invariant ground state) but the triplet band not. The nonbonding band receives a dispersion due to h . It has the maximum (which would correspond to a binding energy maximum in a spectroscopic measurement) at (π, π) . One should note, however, that we did not include into our model all the three oxygen $2p$ orbitals at a given site. There exist other nonbonding oxygen bands and especially that one with lowest binding energy at (π, π) (seen experimentally in Ref. 37) is not present in our model.

Now, we discuss the lowest spin polaron band $\Omega_{\mathbf{k}}$. Comparison of Figs. 1(a) and 1(b) shows that the direct oxygen-oxygen hopping is responsible for the dispersion along the line $(0, \pi) - (\pi, 0)$. The dispersion dependence on frustration in spin subsystem and on temperature was extensively studied in our previous works^{21,26} within an extended basis set. From Fig. 2 we see that the pole strength $Z(\mathbf{k})$ vanishes at the Γ point (with $\mathbf{k} = (0, 0)$). This result is the consequence of a vanishing hybridization between oxygen and copper states at this point. Furthermore, the triplet and the nonbonding oxygen bands are degenerate there. Consequently, all the orbitals which are incorporated into our model give rise to only one oxygen derived peak in the photoemission spectra at the Γ point. And indeed, the spin polaron is not visible in the photoemission spectra there.^{11,37} Note that the vanishing of the hybridization, and consequently the vanishing of the spin polaron is ignored in the course of Emery model reduction to the one-band Hamiltonian (see Refs. 14,33 and references therein), and thus the hole spectral weight is nonzero at $\mathbf{k} = (0, 0)$ in the t - J and other one-band models. Even the theories for the three-band Emery model which start from the Néel order^{9,10} cannot obtain zero spectral weight at $\mathbf{k} = (0, 0)$ since they always deal with a linear combination of states with momentum \mathbf{k} and $\mathbf{k} + \mathbf{q}_0$ ($\mathbf{q}_0 = (\pi, \pi)$).

We note also an apparent similarity of the polaron branch $\Omega_{\mathbf{k}}$ of the present spectrum with the calculations based on the Néel state and linear spin wave theory for t - J ^{2-5,7} and three-band⁸⁻¹⁰ models. However, our results show a slight deviation from the symmetry of the magnetic Brillouin zone $\Omega_{\mathbf{k}} \neq \Omega_{\mathbf{k}+\mathbf{q}_0}$ due to the spin singlet state of the magnetic background. We see from Fig. 1 that the mean field polaron bandwidth $w \sim \tau$ ($w = 2.5\tau$ (2.4τ) for $h = 0$ (0.3τ)). That is larger than expected due to the following reason: in the limit of small $J/\tau \ll 1$ a state $|\mathcal{B}_{\mathbf{k}}\rangle = \mathcal{B}_{\mathbf{k}}^\dagger|\mathcal{G}\rangle$ for a momentum \mathbf{k} near $(0, 0)$ or (π, π) far from the band bottom has an energy $\Omega_{\max} \sim \Omega_{\min} + w$. This energy may be much greater than that of the states

$$|\mathcal{Y}_{\mathbf{k}, \mathbf{q}}\rangle = \tilde{S}_{\mathbf{q}}\mathcal{B}_{\mathbf{k}-\mathbf{q}}^\dagger|\mathcal{G}\rangle$$

where we defined

$$\tilde{S}_{\mathbf{q}} = \frac{1}{\sqrt{N}} \sum_{\mathbf{R}} e^{i\mathbf{q}\mathbf{R}} \tilde{S}_{\mathbf{R}}. \quad (3.15)$$

The energy of the states $|\mathcal{Y}_{\mathbf{k}, \mathbf{q}}\rangle$ is of the order of $\Omega_{\min} + J$ for $\mathbf{k} - \mathbf{q}$ near the band bottom. It means that $|\mathcal{B}_{\mathbf{k}}\rangle$ is unstable with respect to the decay into $|\mathcal{Y}_{\mathbf{k}, \mathbf{q}}\rangle$ states and analogous states, which contain more spinwaves. These states contain spin distortions that are situated far from the hole. In order to take them into account within the PM we should extend the basis set up to infinity. On the other hand the effect of these states can be described by treating the scattering of the spin polaron in terms of irreducible GF, also known as the Tserkovnikov technique. As we will see, this repairs the too large polaron bandwidth in the simple projection method.

4. SCATTERING FOR POLARON GREEN'S FUNCTION

We treat the polaron operator $\mathcal{B}_{\mathbf{k}}^\dagger = \mathcal{B}_{1,\mathbf{k}}^\dagger$ (3.5) as a candidate for the elementary excitation and calculate the corresponding two-time retarded GF $G_p(\mathbf{k}, \omega)$ which is defined in (3.10). The Dyson equation for G_p has the form

$$G_p^{-1}(\mathbf{k}, \omega) = \left[G_p^{(0)} \right]^{-1} - \Sigma(\mathbf{k}, \omega); \quad \Sigma(\mathbf{k}, \omega) = \langle \mathcal{R}_{\mathbf{k}} | \mathcal{R}_{\mathbf{k}}^\dagger \rangle_\omega^{(irr)}, \quad (4.1)$$

with

$$G_p^{(0)} = (\omega - \Omega_{\mathbf{k}})^{-1}; \quad \mathcal{R}_{\mathbf{k}} = [\mathcal{B}_{\mathbf{k}}, H] \quad (4.2)$$

and where we used the irreducible GF

$$\langle \mathcal{R}_{\mathbf{k}} | \mathcal{R}_{\mathbf{k}}^\dagger \rangle_\omega^{(irr)} = \langle \mathcal{R}_{\mathbf{k}} | \mathcal{R}_{\mathbf{k}}^\dagger \rangle_\omega - \langle \mathcal{R}_{\mathbf{k}} | \mathcal{B}_{\mathbf{k}}^\dagger \rangle_\omega \frac{1}{\langle \mathcal{B}_{\mathbf{k}} | \mathcal{B}_{\mathbf{k}}^\dagger \rangle_\omega} \langle \mathcal{B}_{\mathbf{k}} | \mathcal{R}_{\mathbf{k}}^\dagger \rangle_\omega \quad (4.3)$$

in accordance with the definition given by Tserkovnikov.²⁷ The results for $G_p(\mathbf{k}, \omega)$ can be used to calculate $G_h(\mathbf{k}, \omega)$ for low energies

$$G_h(\mathbf{k}, \omega) \approx Z(\mathbf{k}) G_p(\mathbf{k}, \omega). \quad (4.4)$$

It must be underlined that Eq. (4.1) coincides only formally with the Dyson equation for the causal Green's function. The "self-energy" $\Sigma(\mathbf{k}, \omega)$ in (4.1) has no diagrammatic representation and it is represented by more complex Green's functions in the right hand side of Eq. (4.3). The derivation of Eq. (4.3) and its relation to the conventional projection technique^{31,32,38} are represented in Appendix A. As follows from (4.1) $\text{Re } \Sigma$ gives the renormalization of the energy of the polaron $\mathcal{B}_{\mathbf{k}}^\dagger$ and $\text{Im } \Sigma$ gives its damping when $|\text{Im } \Sigma(\mathbf{k}, \omega)| \ll |\text{Re } \Sigma(\mathbf{k}, \omega)|$. In a general case the elementary excitations must be investigated self-consistently. The self-energy $\Sigma(\mathbf{k}, \omega)$ is dictated by the interaction of the polaron with the spin subsystem, i.e., by the polaron scattering on the spin waves. For this reason the main problem of the present technique consists in calculating the irreducible Green's function (4.3).

5. VERTEX CALCULATION

To determine $\mathcal{R}_{\mathbf{k}}$ we have to calculate the commutator with the Hamiltonian. That gives in detail

$$\begin{aligned} [B_{1,\mathbf{k}}, \hat{H}] &= \left(2\tau\beta_{\mathbf{k}}^2 - \frac{8h\pi_{\mathbf{k}}^2}{\beta_{\mathbf{k}}^2} \right) B_{1,\mathbf{k}} + 4\tau\beta_{\mathbf{k}}\nu_{\mathbf{k}}B_{2,\mathbf{k}} - \frac{4h\pi_{\mathbf{k}}\delta_{\mathbf{k}}}{\beta_{\mathbf{k}}^2} B_{3,\mathbf{k}}, \\ [B_{2,\mathbf{k}}, \hat{\tau}] &= \tau \left[3\frac{\beta_{\mathbf{k}}}{\nu_{\mathbf{k}}} B_{1,\mathbf{k}} - 2B_{2,\mathbf{k}} + \frac{2}{\nu_{\mathbf{k}}\sqrt{N}} \sum_{\mathbf{q}} \gamma_{\mathbf{k}-\mathbf{q}} (\beta_{\mathbf{k}-\mathbf{q}} Y_{1,\mathbf{k},\mathbf{q}} + 2\nu_{\mathbf{k}-\mathbf{q}} Y_{2,\mathbf{k},\mathbf{q}}) \right], \\ [B_{2,\mathbf{k}}, \hat{J}] &= 4J \frac{1}{\nu_{\mathbf{k}}\sqrt{N}} \sum_{\mathbf{q}} \gamma_{\mathbf{q}} \sqrt{\frac{2}{3}} \nu_{\mathbf{k}-\mathbf{q}} Y_{J,\mathbf{k},\mathbf{q}}, \\ [B_{2,\mathbf{k}}, \hat{h}] &= -2hB_{2,\mathbf{k}} + \frac{1}{\nu_{\mathbf{k}}\sqrt{N}} \sum_{\mathbf{q}} \left[-\frac{(8h\pi_{\mathbf{k}-\mathbf{q}}^2 - 2h\beta_{\mathbf{k}-\mathbf{q}}^2)}{\beta_{\mathbf{k}-\mathbf{q}}} Y_{1,\mathbf{k},\mathbf{q}} - \frac{4h\pi_{\mathbf{k}-\mathbf{q}}\delta_{\mathbf{k}-\mathbf{q}}}{\beta_{\mathbf{k}-\mathbf{q}}} Y_{3,\mathbf{k},\mathbf{q}} \right], \end{aligned} \quad (5.1)$$

where we introduced the notation

$$Y_{i,\mathbf{k},\mathbf{q}} = \tilde{S}_{\mathbf{q}} B_{i,\mathbf{k}-\mathbf{q}}. \quad (5.2)$$

In the scattering term of the exchange energy \hat{J} arises

$$Y_{J,\mathbf{k},\mathbf{q}} \equiv S_{\mathbf{q}}^{\alpha} \left[\frac{1}{\nu_{\mathbf{k}-\mathbf{q}} \sqrt{\frac{2}{3}N}} \sum_{\mathbf{R}} e^{-i(\mathbf{k}-\mathbf{q})\mathbf{R}} \left(i\epsilon_{\alpha\beta\gamma} S_{\mathbf{R}}^{\beta} \hat{\sigma}^{\gamma} p_{\mathbf{R}} \right) \right]. \quad (5.3)$$

which has a different structure ($\epsilon_{\alpha\beta\gamma}$ is the antisymmetric tensor). Therefore, it has to be projected

$$\left[B_{2,\mathbf{k}}, \hat{J} \right] \approx 4J \frac{1}{\nu_{\mathbf{k}} \sqrt{N}} \sum_{\mathbf{q}} \gamma_{\mathbf{q}} \left(\frac{2}{3} \right) \nu_{\mathbf{k}-\mathbf{q}} Y_{2,\mathbf{k},\mathbf{q}}, \quad (5.4)$$

using

$$\left\langle \left\{ Y_{J,\mathbf{k},\mathbf{q}}, Y_{2,\mathbf{k},\mathbf{q}}^{\dagger} \right\} \right\rangle = \frac{2}{3} C_{\mathbf{q}}; \quad C_{\mathbf{q}} = \sum_{\mathbf{R}} e^{-i\mathbf{q}(\mathbf{n}-\mathbf{R})} \langle S_{\mathbf{n}}^{\alpha} S_{\mathbf{R}}^{\alpha} \rangle. \quad (5.5)$$

Finally one finds

$$\left[B_{3,\mathbf{k}}, \hat{H} \right] = -\frac{4h\pi_{\mathbf{k}} \delta_{\mathbf{k}}}{\beta_{\mathbf{k}}^2} B_{1,\mathbf{k}} + \frac{8h\pi_{\mathbf{k}}^2}{\beta_{\mathbf{k}}^2} B_{3,\mathbf{k}}. \quad (5.6)$$

After carrying out the projection (5.4), all terms $R_{i,\mathbf{k}} \equiv \left[B_{i,\mathbf{k}}, \hat{H} \right]$ can be represented in unique form

$$R_{i,\mathbf{k}} = \lambda_{ij} B_{j,\mathbf{k}} + \frac{1}{\sqrt{N}} \sum_{\mathbf{q}} g_{ij,\mathbf{k},\mathbf{q}} Y_{j,\mathbf{k},\mathbf{q}} \quad (5.7)$$

with coefficients λ_{ij} and $g_{ij,\mathbf{k},\mathbf{q}}$ that can be simply derived from (5.1,5.4) and (5.6). One should note that the scattering has its origin mainly in the second basis operator $B_{2,\mathbf{k}}$ (3.1) since only coefficients $g_{2j,\mathbf{k},\mathbf{q}}$ are different from zero. We find from Eq. (5.7):

$$\mathcal{R}_{\mathbf{k}} = \alpha_i^{(1)}(\mathbf{k}) R_{i,\mathbf{k}} = \alpha_i^{(1)}(\mathbf{k}) \lambda_{ij} B_{j,\mathbf{k}} + \check{R}_{\mathbf{k}}, \quad (5.8)$$

where we define

$$\check{R}_{\mathbf{k}} = \frac{1}{\sqrt{N}} \sum_{\mathbf{q}} \alpha_i^{(1)}(\mathbf{k}) g_{ij,\mathbf{k},\mathbf{q}} Y_{j,\mathbf{k},\mathbf{q}} = \frac{1}{\sqrt{N}} \sum_{\mathbf{q}} \tilde{S}_{\mathbf{q}} \left(\alpha_i^{(1)}(\mathbf{k}) g_{ij,\mathbf{k},\mathbf{q}} B_{j,\mathbf{k}-\mathbf{q}} \right). \quad (5.9)$$

We see from Eqs. (4.1,4.3), that the self-energy $\Sigma(\mathbf{k},\omega)$ accounting for interaction effects is expressed through higher order Green's functions (see Appendix A). One should notice that the terms linear in $\mathcal{B}_{\mathbf{k}} \equiv \mathcal{B}_{1,\mathbf{k}}$ in Eq. (5.8) do not contribute to the irreducible Green's function (4.3) for $\Sigma(\mathbf{k},\omega)$. The terms $\propto \mathcal{B}_{j,\mathbf{k}}$, $j=2,3$, in Eq. (5.8) are orthogonal to $\mathcal{B}_{\mathbf{k}}$ and give nonvanishing contribution to the irreducible Green's function (4.3) only in the energy region of the upper polaron bands. If the lowest polaron band may be regarded as isolated (i.e. if it is energetically well separated from other bands), we can neglect the interband scattering and retain only the intraband one. This is the case in our problem, since the energy gap (1.3τ for $h=0$ and 1.9τ for $h=0.3$, see Fig.1) between the two lowest bands is about half of the mean field bandwidth of the polaron. Then we project the operator $\left(\alpha_i^{(1)}(\mathbf{k}) g_{ij,\mathbf{k},\mathbf{q}} B_{j,\mathbf{k}-\mathbf{q}} \right)$ onto $\mathcal{B}_{\mathbf{k}-\mathbf{q}}$ and obtain finally

$$\check{R}_{\mathbf{k}} \approx \frac{1}{\sqrt{N}} \sum_{\mathbf{q}} \Gamma(\mathbf{k},\mathbf{q}) \tilde{S}_{\mathbf{q}} \mathcal{B}_{\mathbf{k}-\mathbf{q}} \quad (5.10)$$

where

$$\Gamma(\mathbf{k},\mathbf{q}) = \left\langle \left\{ \alpha_i^{(1)}(\mathbf{k}) g_{ij,\mathbf{k},\mathbf{q}} B_{j,\mathbf{k}-\mathbf{q}}, \alpha_i^{(1)}(\mathbf{k}-\mathbf{q}) B_{i,\mathbf{k}-\mathbf{q}}^{\dagger} \right\} \right\rangle = \alpha_i^{(1)}(\mathbf{k}) g_{ij,\mathbf{k},\mathbf{q}} \alpha_j^{(1)*}(\mathbf{k}-\mathbf{q}). \quad (5.11)$$

In the following we will use $\check{R}_{\mathbf{k}}$ instead of $\mathcal{R}_{\mathbf{k}}$ in Eq. (4.3). Then the lowest order self-energy contribution is provided by the first term in the right hand side of the expression (4.3), which is responsible for the

scattering of polarons, while the second term leads to higher order corrections (see the discussion in the Appendix A). One should mention that the operators $Y_{i,\mathbf{k},\mathbf{q}}$ are orthogonal among each other. However, unlike the basis operators (3.1, 3.4) only up to terms of order $1/N$. Therefore, one may obtain artificial terms in the vertex $\Gamma(\mathbf{k}, \mathbf{q})$ if one carries out the calculation in a changed order than that one presented here.

In our previous work^{28,29} we used only one operator in the PM. The present method generalizes the recipe of vertex calculation from Ref. 28 to the more complex case of several operators in the PM basis set.

6. SELF-CONSISTENT BORN APPROXIMATION

The self-energy (4.3) with $\check{R}_{\mathbf{k}}$ (5.10) provides the opportunity to apply the mode-coupling approximation in terms of an independent propagation of the polaron and spin excitations. It consists in the proper decoupling procedure for the two time correlation function

$$\langle \check{R}_{\mathbf{k},\sigma}(t) \check{R}_{\mathbf{k},\sigma}^\dagger(t') \rangle \simeq \frac{1}{N} \sum_{\mathbf{q}} \Gamma^2(\mathbf{k}, \mathbf{q}) \langle \mathcal{B}_{\mathbf{k}-\mathbf{q},\sigma}(t) \mathcal{B}_{\mathbf{k}-\mathbf{q},\sigma}^\dagger(t') \rangle \langle \mathbf{S}_{-\mathbf{q}}(t) \mathbf{S}_{\mathbf{q}}(t') \rangle, \quad (6.1)$$

$$\langle \mathbf{S}_{-\mathbf{q}}(t) \mathbf{S}_{\mathbf{q}}(t') \rangle = \frac{1}{N} \sum_{\mathbf{r}, \mathbf{r}'} e^{i\mathbf{q} \cdot (\mathbf{r}' - \mathbf{r})} \langle \mathbf{S}_{\mathbf{r}}(t) \mathbf{S}_{\mathbf{r}'}(t') \rangle. \quad (6.2)$$

In the frameworks of such a mode-coupling approximation the second term in the right hand side of Eq. (4.3) may be neglected (see the discussion in the Appendix A). The first term $\langle \check{R}_{\mathbf{k}} | \check{R}_{\mathbf{k}}^\dagger \rangle_\omega$ of (4.3) may be expressed in terms of the Fourier transform of the above two-time correlation function (6.1). The presence of the polaron-polaron correlation function $\langle \mathcal{B}_{\mathbf{k}-\mathbf{q}}(t) \mathcal{B}_{\mathbf{k}-\mathbf{q}}^\dagger(t') \rangle$ in the right hand side of Eq. (6.1) allows the self-consistent calculation of $G_p(\mathbf{k}, \omega)$. Note that in the case of the t - J model, investigated in terms of spinless holes, the analogous decoupling procedure for the irreducible Green's function of the form (4.3) is equivalent to SCBA in a usual diagrammatic technique.⁷

The spin-spin correlation function $\langle \mathbf{S}_{-\mathbf{q}}(t) \mathbf{S}_{\mathbf{q}}(t') \rangle$ in (6.1) is calculated from the spin excitation Green's function $D(\mathbf{q}, \omega)$. We treat the spin subsystem in the spherically symmetric approach,²³⁻²⁵ which is briefly described in the Appendix B. The Green's function $D(\mathbf{q}, \omega)$ has the form

$$D(\mathbf{q}, \omega) = \langle S_{-\mathbf{q}}^\alpha | S_{\mathbf{q}}^\alpha \rangle_\omega = -8JC_{\mathbf{g}} \frac{1 - \gamma_{\mathbf{q}}}{\omega^2 - \omega_{\mathbf{q}}^2}; \quad (6.3)$$

$$\omega_{\mathbf{q}}^2 = -32J\alpha_1 (C_{\mathbf{g}}/3) (1 - \gamma_{\mathbf{q}})(2\Delta + 1 + \gamma_{\mathbf{q}}).$$

We neglect the influence of doped holes on the copper spin dynamics and take the spin spectrum parameters calculated in Ref. 25: $\Delta = 0$, for $T = 0$, the vertex correction $\alpha_1 = 2.35$, the spin excitations condensation part $m^2 = 0.09$. Note that the spin excitation spectrum $\omega_{\mathbf{q}}$ has the magnetic BZ symmetry at $\Delta = 0$, but the Green's function $D(\mathbf{q}, \omega)$ has the symmetry of the full BZ due to the numerator $(1 - \gamma_{\mathbf{q}})$.

As a result of the decoupling (6.1) we come to the integral equation for the Green's function

$$G_p(\mathbf{k}, \omega) = \frac{1}{\omega - \Omega_{\mathbf{k}} - \Sigma(\mathbf{k}, \omega)}, \quad (6.4)$$

where

$$\Sigma(\mathbf{k}, \omega) = \frac{1}{N} \sum_{\mathbf{q}} M^2(\mathbf{k}, \mathbf{q}) G_p(\mathbf{k} - \mathbf{q}, \omega - \omega_{\mathbf{q}}), \quad (6.5)$$

$$M^2(\mathbf{k}, \mathbf{q}) = \Gamma^2(\mathbf{k}, \mathbf{q}) \frac{(-4C_{\mathbf{g}})(1 - \gamma_{\mathbf{q}})}{\omega_{\mathbf{q}}}. \quad (6.6)$$

$\Gamma(\mathbf{k}, \mathbf{q})$ corresponds to the bare vertex for the coupling between a spin polaron and a spin wave. It is known^{39,40} that this vertex is substantially renormalized for \mathbf{q} close to the antiferromagnetic vector $\mathbf{q}_0 = (\pi, \pi)$. This renormalization is due to the strong interaction of a polaron with the condensation part of spin excitations that must be taken into account from the very beginning. As a result, the renormalized vertex $\tilde{\Gamma}(\mathbf{k}, \mathbf{q})$ must be proportional to³⁹ $\left[(\mathbf{q} - \mathbf{q}_0)^2 + L_s^{-2} \right]^{1/2}$, L_s being the spin-spin correlation length, $L_s \rightarrow \infty$ in our case of a long range order state of the spin subsystem. Below, this renormalization is taken into account empirically by the substitution

$$\Gamma(\mathbf{k}, \mathbf{q}) \rightarrow \tilde{\Gamma}(\mathbf{k}, \mathbf{q}) = \Gamma(\mathbf{k}, \mathbf{q}) \sqrt{1 + \gamma_{\mathbf{q}}}. \quad (6.7)$$

The introduced vertex correction is proportional to $|\mathbf{q} - \mathbf{q}_0|$ for \mathbf{q} close to \mathbf{q}_0 . Let us mention that the bare vertex leads to a dramatic decrease of the QP bandwidth.

7. RESULTS AND DISCUSSION

In this section we present the results for the low energy part of the one-particle retarded Green's function $G_h(\mathbf{k}, \omega)$ (3.11). In our treatment we ignore the scattering of a polaron to the upper bands. In this approximation the low energy part of $G_h(\mathbf{k}, \omega)$ is related with the polaron Green's function $G_p(\mathbf{k}, \omega)$ through Eq. (4.4). We are mostly interested in the spectral function of the polaron or hole GF, respectively, which are given by

$$A_{p/h}(\mathbf{k}, \omega) = -\frac{1}{\pi} \text{Im} G_{p/h}(\mathbf{k}, \omega). \quad (7.1)$$

The spectral function of a bare hole A_h is roughly proportional to the intensity in an angle resolved photoemission (ARPES) experiment. The self-consistent equation (6.4) was solved by means of the recursive procedure that provides step by step the coefficients a_n, b_n of the continued fraction expansion of $G_p(\mathbf{k}, \omega)$. The details of the calculation will be published elsewhere²⁹. The two-dimensional Simpson's rule was used for the integration in Eq. (6.5) over 231 points in the irreducible part of the Brillouin zone. The prominent feature of the expansion is the fast convergence of coefficients a_n, b_n to the asymptotic behavior which is characterized by a linear dependence on n . The slope for a_n is twice as large as the slope for b_n . This feature allows to use the incomplete gamma function as an analytic terminator⁴¹ for the continued fraction. We applied the terminator after the calculation of 30 pairs of coefficients. Our calculations for various models of strongly correlated electrons indicate that the linear growth of continued fraction coefficients seems to be a common feature of such models.

The solid line in the Figure 1 shows the dispersion $\varepsilon(\mathbf{k})$ of the lowest peak in the spectral density. First, we may see that the overall shape of the dispersion curve has not changed in comparison with the mean field result. On the other hand, we may note that the energy renormalization for the top of the band is larger than for the bottom resulting in substantial narrowing of the band. Although the band width of the polaron in mean field $\Omega_{\mathbf{k}}$ is proportional to the hopping amplitude τ , it is reduced to a band width proportional to J due to the scattering of the polaron at spin fluctuations which are inherent in $\varepsilon(\mathbf{k})$. Let us note that the polaron mean field energy $\Omega_{\mathbf{k}}$ represents the center of gravity of the polaron spectral function $A_p(\mathbf{k}, \omega)$ that is

$$\Omega_{\mathbf{k}} = \int_{-\infty}^{\infty} \omega A_p(\mathbf{k}, \omega) d\omega. \quad (7.2)$$

On the other hand, we see from the explicit expressions for the Liouvillean matrix elements (3.8) that $\Omega_{\mathbf{k}}$ is unambiguously related to the nearest neighbor and next-nearest neighbor static spin-spin correlation functions of the undoped system. The latter is described by the Heisenberg Hamiltonian (2.2) on the

square lattice, and the correlation functions are known at present time with a very high accuracy from various analytic^{24,43} and numerical^{22,42} approaches. That means the asymmetry of $\Omega_{\mathbf{k}}$ (with respect to the magnetic Brillouin zone) is not only a consequence of the particular approximations made in the present work, but already a property of the polaron spectral function itself.

Figure 3 gives the polaron and hole spectral densities for three characteristic momenta \mathbf{k} to distinguish three regimes. In addition, we show the real and imaginary parts of the self-energy $\Sigma(\mathbf{k}, \omega)$ which are approximately identical for polaron or hole GF according to Eq. (4.4). Let us recall that we have made the change $\mathbf{k} \rightarrow \mathbf{k}' = \mathbf{k} - \mathbf{q}_0$ in the final results, so that the quasimomenta in the figures correspond to the actual Brillouin zone of the CuO₂ plane, in contrast to our previous work.²⁸ We find a sharp quasiparticle peak at the bottom of the spectra for $\mathbf{k}_a = (\pi/2, \pi/2)$ and $\mathbf{k}_b = (7\pi/20, 7\pi/20)$. The position of the quasiparticle peak corresponds to the condition $\text{Re } G_p^{-1}(\mathbf{k}, \omega) = 0$, i.e. the point where we have a crossing of the functions $\omega - \Omega_{\mathbf{k}}$ and $\text{Re } \Sigma(\mathbf{k}, \omega)$, see Figs. 3(a) and 3(b). Quite a different shape has the spectral density $A_p(\mathbf{k}_c, \omega)$ at $\mathbf{k}_c = (0, 0)$. Its lowest peak is not related to the zero of $\text{Re } G_p^{-1}(\mathbf{k}, \omega)$ and is due to abrupt changes in the self-energy. That leads to a large imaginary part of $\Sigma(\mathbf{k}, \omega)$ at the position of the lowest peak in the spectral function. We may say that there is *no* quasiparticle excitation for this quasimomentum value.

Figure 4 shows the difference between the quasiparticle excitations at points \mathbf{k}_a and \mathbf{k}_b more in detail. The first one corresponds to a quasiparticle with infinite lifetime, i.e. to an isolated pole of the Green's function at the real axis of the complex energy plane. For \mathbf{k}_b the situation is different, a very small, but finite, imaginary part of the self-energy is present in the region of the peak. The shape of the peak deviates from Lorentzian. Therefore, such an excitation can be regarded as a quasiparticle with finite lifetime.

Table 1 shows the position of the lowest peak, $\varepsilon(\mathbf{k})$, the area under the peak for polaron $W_p(\mathbf{k})$ and for hole spectral function, $W_h(\mathbf{k}) = Z(\mathbf{k}) W_p(\mathbf{k})$ (see (4.4)), and the value of the imaginary part of the self-energy, $-\text{Im } \Sigma[\mathbf{k}, \varepsilon(\mathbf{k})]$ for \mathbf{k} values which vary along the diagonal of the Brillouin zone. The rows which are marked by a star do not represent a quasiparticle excitation like at \mathbf{k}_c and the filled or open circles correspond to momenta with quasiparticles of infinite or finite lifetime, respectively.

So, we may distinguish three qualitatively different kinds of spectral function $A_p(\mathbf{k}, \omega)$ behavior:

(i) The lowest peak tends to a delta function $W_p \delta[\omega - \varepsilon(\mathbf{k})]$, when $\text{Im } \omega \rightarrow 0$ (see Fig.4(a)). We have a quasiparticle, characterized by the excitation energy $\varepsilon(\mathbf{k}) = \Omega_{\mathbf{k}} + \text{Re } \Sigma[\mathbf{k}, \varepsilon(\mathbf{k})]$ with infinite lifetime τ_l , $(1/\tau_l) \equiv -\text{Im } \Sigma[\mathbf{k}, \varepsilon(\mathbf{k})] = 0$. These \mathbf{k} -points are situated near the band minimum \mathbf{k}_{min} . They are marked by solid circles at Fig. 1 and in Table 1.

(ii) The lowest peak has approximate Lorentzian form (see Fig.4(b))

$$A_p(\mathbf{k}, \omega) = -\frac{1}{\pi} \text{Im } G_p(\mathbf{k}, \omega) \approx W_p \frac{(1/\tau_l)}{[\omega - \varepsilon(\mathbf{k})]^2 + (1/\tau_l)^2} + A_{\text{incoh}} \quad (7.3)$$

and corresponds to a quasiparticle with energy $\varepsilon(\mathbf{k}) = \Omega_{\mathbf{k}} + \text{Re } \Sigma[\mathbf{k}, \varepsilon(\mathbf{k})]$, and finite lifetime $(1/\tau_l) \approx -\text{Im } \Sigma[\mathbf{k}, \varepsilon(\mathbf{k})] \ll |\varepsilon(\mathbf{k}) - \varepsilon(\mathbf{k}_{\text{min}})|$. The corresponding \mathbf{k} -values are marked by open circles at Fig. 1 and in Table 1.

(iii) The spectral density is completely incoherent and is of the same order of magnitude as the imaginary part of the self-energy at all ω (see Fig.3(c)). These \mathbf{k} -points are marked by stars.

In order to understand the nature of the polaron damping $(1/\tau_l)$ in (7.3), let us consider a particular \mathbf{k} -value and estimate the imaginary part of the self-energy at a particular ω . Changing the summation variable in (6.5) we can calculate the imaginary part of the self-energy as follows

$$-\text{Im } \Sigma(\mathbf{k}, \omega) = \pi \frac{1}{N} \sum_{\mathbf{q}'} M^2(\mathbf{k}, \mathbf{k} - \mathbf{q}') A_p(\mathbf{q}', \omega - \omega_{\mathbf{k}-\mathbf{q}'}). \quad (7.4)$$

Now we suppose that the lowest peak at all $\mathbf{q}' = \mathbf{k} - \mathbf{q}$ may be described approximately by Lorentzian (7.3). Then we see from Eq. (7.4) that large damping, characterized by a large value of $-\text{Im } \Sigma(\mathbf{k}, \omega)$ may only arise when the condition

$$\omega - \varepsilon(\mathbf{q}') - \omega_{\mathbf{k}-\mathbf{q}'} = 0 \quad (7.5)$$

is satisfied for some values of \mathbf{q}' (see also Ref. 14). On the contrary, if Eq. (7.5) does not hold even at the lowest edge of the spectral function $\omega = \varepsilon(\mathbf{k})$, the damping is absent. In Fig.5 we plot $\varepsilon(\mathbf{q}')$ together with the curve $\varepsilon(\mathbf{k}) - \omega_{\mathbf{k}-\mathbf{q}'}$ for various values of \mathbf{k} (for $h = 0.3\tau$ and where we choose only one direction for both \mathbf{k} , and \mathbf{q}'). We may see that for $\mathbf{k}_{\min} = (\pi/2, \pi/2)$ the condition (7.5) holds only for the trivial values $\mathbf{q} = \mathbf{k} - \mathbf{q}' = (0, 0)$ and $\mathbf{q} = \mathbf{q}_0$, where, however, the vertex $M^2(\mathbf{k}, \mathbf{q})$ vanishes. It demonstrates that it is impossible to scatter from \mathbf{k}_{\min} into other states. The same situation occurs for some finite region of \mathbf{k} values around the band bottom. These are exactly those momenta with a quasiparticle of infinite lifetime. Different is the situation for $\mathbf{k} = (0, 0)$ and $\mathbf{k} = (4\pi/20, 4\pi/20)$ where several nontrivial intersections take place.

Figure 6 shows the low energy part of the hole spectral density $A_h(\mathbf{k}, \omega)$ for \mathbf{k} along high symmetry directions. Let us recall that the intensity of the lowest peak of $A_h(\mathbf{k}, \omega)$ is governed by two circumstances: the \mathbf{k} -dependence of the mean field residue $Z(\mathbf{k})$ (see Eq. (3.12) and the discussion about Fig. 2) and the intensity of the lowest polaron peak of $A_p(\mathbf{k}, \omega)$. One can clearly observe a well defined quasiparticle peak near the bottom of the spectrum at $(\pi/2, \pi/2)$, everywhere along the line $(0, \pi)$ - $(\pi, 0)$ and also near to $(\pi, 0)$. At the Γ -point $(0, 0)$, there is no hole spectral density due to the vanishing residue for the hole Green's function in the lowest mean field polaron band. At the same time one observes intensity at (π, π) . A clear asymmetry of the peak intensity is seen along the diagonal of the BZ. The abrupt drop of the peak intensity in the region $(\pi/2, \pi/2)$ - (π, π) is related to the strong polaron damping there. In other words, most of the mean field hole spectral weight ($Z(\mathbf{k})$ in Fig.2) goes into the incoherent part of the spectrum (situated at higher energies) due to the strong coupling of the polaron $\mathcal{B}_{\mathbf{k}}$ with spin excitations. An analogous behavior of the quasiparticle peak intensity was obtained in Ref. 15 within a variational ansatz for the t - J model.

Let us compare the results with those of the usual SCBA of spinless holes in the pure t - J model. There, one finds quasiparticles with infinite lifetime and finite weight everywhere in \mathbf{k} -space. Additionally, the spectral function has the symmetry of the magnetic BZ. Introducing additional hopping terms (corresponding to direct oxygen-oxygen hopping in the Emery model) leads to a scattering mechanism such that the upper parts of the spectrum loose their quasiparticle character.^{13,14} On the contrary, in our approach, the damping of the spin polaron is already present without direct oxygen-oxygen hopping. If we consider only the dispersion relation $\varepsilon(\mathbf{k})$ we observe a remarkable similarity between the present calculation and earlier results using the SCBA of spinless holes or other methods. In fact, the deviations from the magnetic BZ symmetry in Fig. 1 are not very large. On the other hand, we find some qualitatively new features of the spectral function which are absent in the numerical results of Refs. 5,7. Besides the strong polaron scattering away from the band bottom we note especially: (i) the absence of the polaron quasiparticle at the Γ -point and (ii) the asymmetry of the peak intensity with respect to the magnetic BZ.

Our results (Fig. 6) can also be summarized in such a way that a well pronounced polaron quasiparticle peak exists only around the bottom of the band. In the direction $(\pi/2, \pi/2)$ - $(\pi, 0)$ it is more clearly seen than perpendicular to it. The recent experimental finding³⁷ shows, indeed, that the Zhang-Rice singlet can be observed in $\text{Sr}_2\text{CuO}_2\text{Cl}_2$ only in a similar region of the BZ. And also the higher peak intensity going from $(\pi/2, \pi/2)$ to the Γ -point in comparison with the opposite direction is in agreement with experiment. So we see that those details in which our calculation differs from the standard one^{2,3,5-7} are essential for a better understanding of the experiment.

Let us emphasize that for a detailed comparison to a real experiment there are a considerable number of complications which have not been taken into account in the present work: First, in general a photohole can be generated also on copper, and there will be (in general \mathbf{k} -dependent) interference between the photoholes created on different atoms. An operator $c_{\mathbf{R}+\mathbf{a}}^\dagger$ (2.5) that enters the spin-fermion Hamiltonian (2.1) creates a hole in a state that is an antibonding (in hole notation) combination of oxygen p_σ state and singly occupied copper $d_{x^2-y^2}$ state at adjacent sites. In a more realistic theory one should deal with a complete set of bare oxygen and copper hole creation operators. This may be expected to have some influence on the spectral weight. Next, one must take into account interference terms like $\langle p_x | p_y \rangle$, because the photoemission operator is in general a linear combination of p_x and p_y . Thereby the relative phase between p_x and p_y depends on the momentum transfer, and is in general even different whether one is in the 1st or 2nd Brillouin zone etc. Clearly this will give additional momentum dependence of the weight. Moreover, it is not even a priori clear that p_x and p_y have equal weight in the PES-operator.

Rather this depends in a relatively complicated way, e.g., on the polarization of the incoming X-ray photons. It is in fact well known experimentally that the spectra depend quite sensitively on the X-ray polarization in several oxychlorides like $\text{Sr}_2\text{CuO}_2\text{Cl}_2$ or $\text{Ba}_2\text{Cu}_3\text{O}_4\text{Cl}_2$.^{36,44} At the present stage of many-body theory it is impossible to take all these complications into account. Thus, our comparison with experiment has only qualitative character. Nevertheless, we point out that according to our results, many features of the experimental spectra may originate from the peculiarities of the correlated ground state of the material rather than from the above complications.

We may consider now what happens if we begin to dope our system. First, we suppose that for extremely small doping the Fermi surface will consist of hole pockets centered at $(\pi/2, \pi/2)$. The small spectral weight of the quasiparticle poles in this region means that the surface enclosed inside the Fermi surface may be much larger than the number of holes. Note that due to the strong weight asymmetry the experimental observation of the Fermi surface parts facing M point with $\mathbf{k} = (\pi, \pi)$ point may be very hard to do. In Ref. 45 the observation of weak features in photoemission spectra in this region of \mathbf{k} -space was reported, but the authors can not unambiguously interpret them as Fermi surface cuts. With the increase of doped holes the antiferromagnetic correlations in the spin subsystem are weakened resulting in a deformation of the hole dispersion.^{26,46} The minimum of the hole spectrum should shift to the M point and a 'large' Fermi surface develops. An analogous scenario was also developed in Ref. 40.

8. CONCLUSION

We proposed a new method to calculate the spectral function of the Emery model in its spin-fermion form combining the Mori-Zwanzig projection method with a representation of the self-energy by irreducible GF. Self-energy effects reduce the mean field bandwidth of the spin polaron to a realistic bandwidth of the order of $2J$, but do not change the overall shape of the dispersion. Direct oxygen-oxygen hopping leads to a more isotropic band minimum around $(\pi/2, \pi/2)$. The quasiparticle weight is maximal (about 0.25) around the minimum of the dispersion. Despite some similarities, we observed several new features of the spectral function which are not present in the usual SCBA^{2,3,5-7} for spinless holes coupled to spinons in the pure t - J model, namely the absence of quasiparticle weight at the Γ point, the strong damping away from the minimum and the asymmetry with respect to the antiferromagnetic BZ (where the asymmetry is present, however, in other approaches to the t - J model)^{15,16}. Qualitatively, these features can be observed in the ARPES experiments on $\text{Sr}_2\text{CuO}_2\text{Cl}_2$. We studied in detail possible damping processes of the spin polaron and distinguished three regions in \mathbf{k} -space where the spin polaron exists with infinite lifetime, finite lifetime or does not exist at all.

ACKNOWLEDGEMENTS

We are grateful to H. Eschrig and L.B. Litinski for valuable discussions and comments. This work was supported, in part, by the INTAS-RFBR (project No. 95-0591), by RSFR (Grants No. 98-02-17187 and 98-02-16730), by Russian National program on Superconductivity (Grant No. 93080), ISI Foundation and EU NTAS Network 1010-CT930055. R.O.K. thanks the Max Planck Arbeitsgruppe Elektronensysteme, in the Technische Universität Dresden for hospitality during accomplishing of this work.

Appendix A

Here we give the derivation of the Tserkovnikov expression for the self-energy (4.3) and compare it with the conventional projection technique expression. We use the equation of motion for the retarded Green's function $G_p(\mathbf{k}, \omega) = \langle \mathcal{B}_{\mathbf{k}} | \mathcal{B}_{\mathbf{k}}^\dagger \rangle_\omega$ (3.10)

$$\omega \langle \mathcal{B}_{\mathbf{k}} | \mathcal{B}_{\mathbf{k}}^\dagger \rangle_\omega = 1 + \langle \mathcal{R}_{\mathbf{k}} | \mathcal{B}_{\mathbf{k}}^\dagger \rangle_\omega = 1 + \langle \mathcal{B}_{\mathbf{k}} | \mathcal{R}_{\mathbf{k}}^\dagger \rangle_\omega. \quad (\text{A.1})$$

Multiplying the equation for the higher order GF

$$\omega \langle \mathcal{R}_{\mathbf{k}} | \mathcal{B}_{\mathbf{k}}^\dagger \rangle_\omega = \langle \{ \mathcal{R}_{\mathbf{k}}, \mathcal{B}_{\mathbf{k}}^\dagger \} \rangle + \langle \mathcal{R}_{\mathbf{k}} | \mathcal{R}_{\mathbf{k}}^\dagger \rangle_\omega$$

by $\langle \mathcal{B}_{\mathbf{k}} | \mathcal{B}_{\mathbf{k}}^\dagger \rangle_\omega$, and noting that $\langle \{ \mathcal{R}_{\mathbf{k}}, \mathcal{B}_{\mathbf{k}}^\dagger \} \rangle = \Omega_{\mathbf{k}}$, we have

$$\omega \langle \mathcal{R}_{\mathbf{k}} | \mathcal{B}_{\mathbf{k}}^\dagger \rangle_\omega \langle \mathcal{B}_{\mathbf{k}} | \mathcal{B}_{\mathbf{k}}^\dagger \rangle_\omega = \Omega_{\mathbf{k}} \langle \mathcal{B}_{\mathbf{k}} | \mathcal{B}_{\mathbf{k}}^\dagger \rangle_\omega + \langle \mathcal{R}_{\mathbf{k}} | \mathcal{R}_{\mathbf{k}}^\dagger \rangle_\omega \langle \mathcal{B}_{\mathbf{k}} | \mathcal{B}_{\mathbf{k}}^\dagger \rangle_\omega. \quad (\text{A.2})$$

In the left-hand side we use the second equality (A.1) to obtain

$$\langle \mathcal{R}_{\mathbf{k}} | \mathcal{B}_{\mathbf{k}}^\dagger \rangle_\omega = \Omega_{\mathbf{k}} \langle \mathcal{B}_{\mathbf{k}} | \mathcal{B}_{\mathbf{k}}^\dagger \rangle_\omega + \langle \mathcal{R}_{\mathbf{k}} | \mathcal{R}_{\mathbf{k}}^\dagger \rangle_\omega \langle \mathcal{B}_{\mathbf{k}} | \mathcal{B}_{\mathbf{k}}^\dagger \rangle_\omega - \langle \mathcal{R}_{\mathbf{k}} | \mathcal{B}_{\mathbf{k}}^\dagger \rangle_\omega \langle \mathcal{B}_{\mathbf{k}} | \mathcal{R}_{\mathbf{k}}^\dagger \rangle_\omega, \quad (\text{A.3})$$

and substitute it into first equality (A.1). Finally Eq. (A.1) takes the form

$$[\omega - \Omega_{\mathbf{k}} - \Sigma(\mathbf{k}, \omega)] G_p(\mathbf{k}, \omega) = 1 \quad (\text{A.4})$$

with the self energy given by (4.3).

In order to clarify the physical meaning of this expression let us compare it with the close expression for $\Sigma_{PT}(\mathbf{k}, \omega)$ which follows from the projection technique (see Refs. 31,32,38). Taking the usual notations for the scalar product in the operator space, the projection operators P and Q and the Liouvillean superoperator \mathcal{L}

$$(A | B) = \langle \{A, B\} \rangle, \quad P = | \mathcal{B}_{\mathbf{k}}^\dagger \rangle \langle \mathcal{B}_{\mathbf{k}} |, \quad Q = 1 - P, \quad \mathcal{L}A = [H, A], \quad A\mathcal{L} = [A, H], \quad (\text{A.5})$$

Green's function and the self-energy may be written as

$$\begin{aligned} G_p(\mathbf{k}, \omega) &= (\mathcal{B}_{\mathbf{k}} | \frac{1}{\omega - \mathcal{L}} \mathcal{B}_{\mathbf{k}}^\dagger) = (\mathcal{B}_{\mathbf{k}} \frac{1}{\omega - \mathcal{L}} | \mathcal{B}_{\mathbf{k}}^\dagger). \\ \Sigma_{PT}(\mathbf{k}, \omega) &= (\mathcal{B}_{\mathbf{k}} | \mathcal{L}Q \frac{1}{\omega - \mathcal{L}Q} \mathcal{L}\mathcal{B}_{\mathbf{k}}^\dagger) = (\mathcal{B}_{\mathbf{k}}\mathcal{L}Q | \frac{1}{\omega - Q\mathcal{L}Q} Q\mathcal{L}\mathcal{B}_{\mathbf{k}}^\dagger), \end{aligned} \quad (\text{A.6})$$

The Tserkovnikov expression (4.3) has the following form in the projection technique notation

$$\begin{aligned} \Sigma_T(\mathbf{k}, \omega) &= (\mathcal{B}_{\mathbf{k}}\mathcal{L} | \frac{1}{\omega - \mathcal{L}} \mathcal{L}\mathcal{B}_{\mathbf{k}}^\dagger) - (\mathcal{B}_{\mathbf{k}}\mathcal{L} | \frac{1}{\omega - \mathcal{L}} \mathcal{B}_{\mathbf{k}}^\dagger) \frac{1}{(\mathcal{B}_{\mathbf{k}} | \frac{1}{\omega - \mathcal{L}} \mathcal{B}_{\mathbf{k}}^\dagger)} (\mathcal{B}_{\mathbf{k}} | \frac{1}{\omega - \mathcal{L}} \mathcal{L}\mathcal{B}_{\mathbf{k}}^\dagger) = \\ &= (\mathcal{B}_{\mathbf{k}}\mathcal{L}Q | \frac{1}{\omega - \mathcal{L}} Q\mathcal{L}\mathcal{B}_{\mathbf{k}}^\dagger) - (\mathcal{B}_{\mathbf{k}}\mathcal{L}Q | \frac{1}{\omega - \mathcal{L}} \mathcal{B}_{\mathbf{k}}^\dagger) \frac{1}{(\mathcal{B}_{\mathbf{k}} | \frac{1}{\omega - \mathcal{L}} \mathcal{B}_{\mathbf{k}}^\dagger)} (\mathcal{B}_{\mathbf{k}} | \frac{1}{\omega - \mathcal{L}} Q\mathcal{L}\mathcal{B}_{\mathbf{k}}^\dagger). \end{aligned} \quad (\text{A.7})$$

In the last equality we excluded the terms linear in $\mathcal{B}_{\mathbf{k}}$. Now we see, that the first term in $\Sigma_T(\mathbf{k}, \omega)$ describes the propagation of a "fluctuation" $\mathcal{B}_{\mathbf{k}}\mathcal{L}Q$ in the full Liouvillean space, and the second counter-term eliminates items corresponding to the propagation in the subspace spanned by $\mathcal{B}_{\mathbf{k}}$, i.e., it makes the same job as the projectors Q surrounding \mathcal{L} in the denominator of $\Sigma_{PT}(\mathbf{k}, \omega)$ (A.6). Using the known rules of matrix algebra it is in fact easy to see that $\Sigma_{PT}(\mathbf{k}, \omega)$ (A.6) is equivalent to $\Sigma_T(\mathbf{k}, \omega)$ (A.7). When we consider only intraband scattering we approximate $\mathcal{B}_{\mathbf{k}}\mathcal{L}Q \approx \tilde{R}_{\mathbf{k}}$, with $\tilde{R}_{\mathbf{k}}$, given by Eq. (5.10). Then our set of approximations is equivalent to the mode-coupling approximation in the projection technique.⁴⁷

Appendix B

Now we review briefly the Kondo-Yamaji theory²³ for an isotropic Heisenberg spin-half antiferromagnet on a square lattice.^{24,25}

In the absence of holes our Hamiltonian reduces to the spin Hamiltonian \hat{J} (2.2). We search the retarded spin-spin Green's function $D(\mathbf{q}, \omega) \equiv \langle S_{\mathbf{q}}^{\alpha} | S_{-\mathbf{q}}^{\alpha} \rangle_{\omega}$ taking into account that $\langle S_{\mathbf{R}}^{\alpha} \rangle \equiv 0$ and $\langle S_{\mathbf{R}}^{\alpha} S_{\mathbf{R}+\mathbf{r}}^{\beta} \rangle = \frac{1}{3} \delta^{\alpha\beta} C_{\mathbf{r}}$ in the adopted spherically symmetric approach. Then we have the following equations of motion for the spin Green's functions

$$\omega \langle S_{\mathbf{q}}^{\alpha} | S_{-\mathbf{q}}^{\alpha} \rangle_{\omega} = \frac{1}{N} \sum_{\mathbf{n}, \mathbf{m}} e^{i\mathbf{q}(\mathbf{n}-\mathbf{m})} \left[J \epsilon_{\alpha\beta\gamma} \sum_{\mathbf{g}} \langle S_{\mathbf{n}+\mathbf{g}}^{\beta} S_{\mathbf{n}}^{\gamma} | S_{\mathbf{m}}^{\alpha} \rangle_{\omega} \right] \quad (\text{B.1})$$

$$\omega \frac{1}{N} \sum_{\mathbf{n}, \mathbf{m}} e^{i\mathbf{q}(\mathbf{n}-\mathbf{m})} J \epsilon_{\alpha\beta\gamma} \sum_{\mathbf{g}} \langle S_{\mathbf{n}+\mathbf{g}}^{\beta} S_{\mathbf{n}}^{\gamma} | S_{\mathbf{m}}^{\alpha} \rangle_{\omega} = zJ |C_{\mathbf{g}}| (1 - \gamma_{\mathbf{q}}) + \frac{1}{2} z J^2 (1 - \gamma_{\mathbf{q}}) \omega \langle S_{\mathbf{q}}^{\alpha} | S_{-\mathbf{q}}^{\alpha} \rangle_{\omega} +$$

$$J^2 \frac{1}{N} \sum_{\mathbf{n}, \mathbf{m}} e^{i\mathbf{q}(\mathbf{n}-\mathbf{m})} \sum_{\substack{\beta \neq \alpha \\ \mathbf{g}_1 \neq \mathbf{g}}} \langle S_{\mathbf{n}}^{\beta} S_{\mathbf{n}+\mathbf{g}}^{\beta} S_{\mathbf{n}+\mathbf{g}-\mathbf{g}_1}^{\alpha} + S_{\mathbf{n}+\mathbf{g}}^{\beta} S_{\mathbf{n}+\mathbf{g}_1}^{\beta} S_{\mathbf{n}}^{\alpha} - (S_{\mathbf{n}}^{\beta} S_{\mathbf{n}+\mathbf{g}_1}^{\beta} + S_{\mathbf{n}+\mathbf{g}-\mathbf{g}_1}^{\beta} S_{\mathbf{n}}^{\beta}) S_{\mathbf{n}+\mathbf{g}}^{\alpha} | S_{\mathbf{m}}^{\alpha} \rangle_{\omega} \\ \approx zJ |C_{\mathbf{g}}| (1 - \gamma_{\mathbf{q}}) + \left[J^2 z^2 \frac{2}{3} |C_{\mathbf{g}}| \alpha_1 (1 - \gamma_{\mathbf{q}}) (2\Delta + 1 + \gamma_{\mathbf{q}}) \right] \langle S_{\mathbf{q}}^{\alpha} | S_{-\mathbf{q}}^{\alpha} \rangle_{\omega} \quad (\text{B.2})$$

$z = 4$ is the coordination number. The last approximate equality was obtained by the unique decoupling procedure for three-site (on different sites) spin-operators:

$$S_{\mathbf{n}_1}^{\beta} S_{\mathbf{m}}^{\beta} S_{\mathbf{l}}^{\alpha} \approx \frac{1}{3} \alpha_{1(2)} C_{\mathbf{n}-\mathbf{m}} S_{\mathbf{l}}^{\alpha}, \quad \beta \neq \alpha. \quad (\text{B.3})$$

Here the parameters α_1 or α_2 are used for the first and the second nearest neighbors \mathbf{n} and \mathbf{m} accordingly. They are regarded as vertex corrections which have to be introduced in order to prevent the violation of the sum rule of the correlation function. The energy gap parameter equals

$$2\Delta = \frac{\alpha_2 \sum_{\mathbf{g}, \mathbf{g}_1} C_{\mathbf{g}+\mathbf{g}_1}}{\alpha_1 z^2 |C_{\mathbf{g}}|} - \frac{\alpha_2 - 1}{\alpha_1} \frac{1}{2z |C_{\mathbf{g}}|} - \frac{z - 1}{z}. \quad (\text{B.4})$$

The substitution of Eq. (B.2) into Eq. (B.1) provides $D(\mathbf{q}, \omega)$ in the form (6.3). The static correlation functions $C_{\mathbf{r}} = \langle S_{\mathbf{R}} S_{\mathbf{R}+\mathbf{r}} \rangle$ may be expressed through $D(\mathbf{q}, \omega)$:

$$C_{\mathbf{r}} = \frac{1}{N} \sum_{\mathbf{q}} e^{-i\mathbf{q}\mathbf{r}} \int_{-\infty}^{\infty} d\omega \frac{[-\text{Im } D(\mathbf{q}, \omega) / \pi]}{\exp(\omega/T) - 1} = \frac{1}{N} \sum_{\mathbf{q}} e^{-i\mathbf{q}\mathbf{r}} \left[-zJ C_{\mathbf{g}} (1 - \gamma_{\mathbf{q}}) \frac{\coth(\omega_{\mathbf{q}}/2T)}{\omega_{\mathbf{q}}} \right] \quad (\text{B.5})$$

For $\mathbf{r} = \mathbf{0}$, $C_{\mathbf{0}} = 3/4$, and the equation (B.5) gives the sum rule for $D(\mathbf{q}, \omega)$. Thus we obtain the set of self-consistent equations (6.3),(B.5). Detailed considerations show that it is overdetermined²⁴ and one extra condition may be imposed to solve it. This condition is the relation between α_1 and α_2 given below. In a macroscopic system ($N \rightarrow \infty$) long-range-order is present for $T = 0$. We have $\Delta = 0$,

$$\omega_{\mathbf{q}} = zJ (2\alpha_1 |C_{\mathbf{g}}| / 3)^{1/2} \sqrt{1 - \gamma_{\mathbf{q}}^2}, \quad m^2 = \lim_{\mathbf{r} \rightarrow \infty} e^{i\mathbf{q}_0 \mathbf{r}} C_{\mathbf{r}} \neq 0.$$

The set (B.5) reduces to

$$C_{\mathbf{r}} = \frac{1}{N} \sum_{\mathbf{q} \neq \mathbf{q}_0} e^{-i\mathbf{q}\mathbf{r}} \left[-\frac{zJ C_{\mathbf{g}} (1 - \gamma_{\mathbf{q}})}{\omega_{\mathbf{q}}} \right] + e^{-i\mathbf{q}_0 \mathbf{r}} m^2. \quad (\text{B.6})$$

Shimahara and Takada²⁴ explored various kinds of extra conditions to determine the parameter's values and found m to be the most sensitive quantity. They proposed to fix $r_\alpha = (\alpha_1 - 1) / (\alpha_2 - 1) = 0.82579$ for all temperatures which gives $m = 0.3$ for $T = 0$. Then the values of ground state energy and uniform spin susceptibility agree with other theories and Monte-Carlo simulations within few percents. For finite temperature the KY theory leads to the absence of LRO and provides a spin susceptibility which has a satisfactory behavior over the whole temperature region: it has a zero temperature derivative at $T = 0$, it exhibits a peak around $T \sim J$ and reproduces the high temperature expansion for $T \geq 1.6J$. In the absence of LRO, the low lying excitations are essentially spin waves propagating in a short-range order with a temperature dependent correlation length. On the other hand, if there exists LRO, the usual spin wave excitations are recovered.

- ¹ E. Dagotto, Rev. Mod. Phys. **66**, 763 (1994).
- ² S. Schmitt-Rink, C.M. Varma, and A.E. Ruckenstein, Phys. Rev. Lett. **60**, 2793 (1988).
- ³ C.L. Kane, P.A. Lee, and N. Read, Phys. Rev. B **39**, 6880 (1989).
- ⁴ R. Eder, and K. Becker, Z. Phys. B **78**, 219 (1990).
- ⁵ G. Martinez, and P. Horsch, Phys. Rev. B **44**, 317 (1991).
- ⁶ Z. Liu, E. Manousakis, Phys. Rev. B **45**, 2425 (1992).
- ⁷ N.M. Plakida, V.S. Oudovenko, and V.Yu. Yushankhai, Phys. Rev. B **50**, 6431 (1994).
- ⁸ R. Eder, K. Becker, Z. Phys. B **79**, 333 (1990).
- ⁹ V.V. Kabanov and A. Vagov, Phys. Rev. B **47**, 12134 (1993).
- ¹⁰ O.A. Starykh, O.F. de Alcantara Bonfim, and G.F. Reiter, Phys. Rev. B **52**, 12534 (1995).
- ¹¹ B.O. Wells, Z.-X. Shen, A. Matsuura, D.M. King, M.A. Kastner, M. Greven, and R.J. Birgeneau, Phys. Rev. Lett. **74**, 964 (1995).
- ¹² A. Nazarenko, K.J.E. Vos, S. Haas, E. Dagotto, and R.J. Gooding, Phys. Rev. B **51**, 8676 (1995).
- ¹³ J. Bala, A. Oleś, and J. Zaanen, Phys. Rev. B **52**, 4597 (1995).
- ¹⁴ V.Yu. Yushankhai, V.S. Oudovenko, and R. Hayn, Phys. Rev. B **55** (1997).
- ¹⁵ R. Eder, and K. Becker, Phys. Rev. B **44**, 6982 (1991).
- ¹⁶ H. Eskes, and R. Eder, Phys. Rev. B **54**, R14226 (1996).
- ¹⁷ K.J.E. Vos, and R.J. Gooding, Z. Phys. B **101**, 79 (1996).
- ¹⁸ V.J. Emery, Phys. Rev. Lett. **58**, 2794 (1988).
- ¹⁹ V.J. Emery, and G. Reiter, Phys. Rev. B **38**, 4547 (1988).
- ²⁰ A.F. Barabanov, L.A. Maksimov, and G.V. Uimin, Pisma v Zh. Eksp. Teor. Fiz. **47**, 532 (1988) [JETP Lett. **47**, 622 (1988)]; Zh. Eksp. Teor. Fiz. **96**, 655 (1989) [JETP **69**, 371 (1989)].
- ²¹ A.F. Barabanov, R.O. Kuzian, and L.A. Maksimov, J. Phys. Cond. Matter **3**, 9129 (1991).
- ²² S. Liang, B. Doucot, and P.W. Anderson, Phys. Rev. Lett. **61**, 365 (1988).
- ²³ J. Kondo, and K. Yamaji, Prog. Theor. Phys. **47**, 807 (1972).
- ²⁴ H. Shimahara, and S. Takada, J. Phys. Soc. Jpn. **60**, 2394 (1991).
- ²⁵ A.F. Barabanov, and O. Starykh, J. Phys. Soc. Jpn. **61**, 704 (1992); A.F. Barabanov, and V.M. Berezovsky, Zh. Eksp. Teor. Fiz. **106**, 1156 (1994) [JETP **79** (4), 627 (1994)]; J. Phys. Soc. Jpn. **63**, 3974 (1994).
- ²⁶ A.F. Barabanov, V.M. Berezovsky, E.Žasinas, and L.A. Maksimov, Zh. Eksp. Teor. Fiz. **110**, 1480 (1996) [JETP **83**, 819 (1996)].
- ²⁷ Yu.A. Tserkovnikov, Teor. Mat. Fiz. **49**, 219 (1981) [in english: 993 (1982)].
- ²⁸ A.F. Barabanov, R.O. Kuzian, and L.A. Maksimov, Phys. Rev. B **55**, 4015 (1997).
- ²⁹ A.F. Barabanov, R.O. Kuzian, L.A. Maksimov, and E.Žasinas, to appear in Zh. Eksp. Teor. Fiz. (1998) [JETP (1998)].
- ³⁰ J. Zaanen, and A.M. Oleś, Phys. Rev. B **37**, 9423 (1988).
- ³¹ H. Mori, Prog. Theor. Phys. **33**, 423 (1965).
- ³² P.Fulde, *Electronic correlations in Molecules and Solids*, Berlin, Springer, 1995.
- ³³ F.C. Zhang, and T.M. Rice, Phys. Rev. B **37**, 3759 (1988).
- ³⁴ D.N. Zubarev, Usp. Fiz. Nauk **71**, 71 (1960) [Sov. Phys. Uspekhi **3**, 320 (1960)].
- ³⁵ H. Eskes, L.H. Tjeng, and G.A. Sawatzky, Phys. Rev. B **41**, 288 (1990).

- ³⁶ H.C. Schmelz, M.S. Golden, S. Haffner, M. Knupfer, G. Krabbes, J. Fink, H. Rosner, R. Hayn, H. Eschrig, A. Müller, Ch. Jung, and G. Reichardt, Phys. Rev. B, *in print*.
- ³⁷ J.J.M. Pothuizen, R. Eder, M. Matoba, G.A. Sawatzky, N.T. Hien, and A.A. Menovsky, Phys. Rev. Lett. **78**, 717 (1997).
- ³⁸ D. Forster, *Hydrodynamic Fluctuations, Broken Symmetry and Correlation Functions* (Reading, MA: Benjamin, 1975).
- ³⁹ J.R. Schrieffer, J. Low. Temp. Phys. **99**, 397 (1995).
- ⁴⁰ A.V. Chubukov, and D.K. Morr, cond-mat/9701196
- ⁴¹ R. Haydock, and C.M.M. Nex, J. Phys. C: Solid State Phys. **18** (1985) 2235.
- ⁴² J. Oitmaa, and D.D. Betts, Can. J. Phys. **56**, 897 (1978).
- ⁴³ K.W. Becker, H. Won and P. Fulde, Z. Phys. B **75**, 335 (1989).
- ⁴⁴ M.S. Golden, H.C. Schmelz, M. Knupfer, S. Haffner, G. Krabbes, J. Fink, V.Yu. Yushankhai, H. Rosner, R. Hayn, A. Müller, and G. Reichardt, Phys. Rev. Lett. **78**, 4107 (1997).
- ⁴⁵ D.S. Marshall, D.S. Dessau, A.G. Loeser, C.-H. Park, A.Y. Matsuura, J.N. Eckstein, I. Bozovic, P. Fournier, A. Kapitulnik, W.E. Spicer, and Z.X. Shen, Phys. Rev. Lett. **76**, 4841 (1996).
- ⁴⁶ R. Hayn, J.L. Richard, and V.Yu. Yushankhai, Solid State Commun. (1994), R. Hayn, A.F. Barabanov, J. Schulenburg, Z. Phys. B **102**, 359 (1997).
- ⁴⁷ V.L. Aksenov, M. Bobeth, N.M. Plakida, and J. Schreiber, J. Phys. C: Solid State Phys. **20**, 375 (1987).

FIG. 1. The dispersion of the lowest QP band $\varepsilon(\mathbf{k})$ and the mean field dispersions $\Omega_{\mathbf{k}}^{(i)}$ along high symmetry lines in the Brillouin zone for $J = 0.2$ and $\tau = 1$ without (a, $h = 0$) and with (b, $h = 0.3$) direct oxygen-oxygen hopping. Filled and open circles mark quasiparticles with infinite and finite lifetime, respectively. A star corresponds to a lowest peak in the spectral density which is strongly overdamped. The points in \mathbf{k} space mean: $\Gamma = (0, 0)$, $X = (\pi, 0)$, $M = (\pi, \pi)$ and $X' = (0, \pi)$.

FIG. 2. The QP weights $Z^{(i)}(\mathbf{k})$ of all three bands in the projection method (PM) and the area under the lowest peak of the hole spectral function $W_h(\mathbf{k})$ calculating the irreducible GF of the self-energy in self-consistent Born approximation (SCBA) along high symmetry lines in the Brillouin zone for $J = 0.2$ and $\tau = 1$ without (a, $h = 0$) and with (b, $h = 0.3$) direct oxygen-oxygen hopping.

FIG. 3. Polaron and hole spectral densities $A_{p/h}(\mathbf{k}, \omega)$ around the lowest peak for the momenta: a) $\mathbf{k} = (\pi/2, \pi/2)$, b) $\mathbf{k} = 7(\pi/20, \pi/20)$ and c) $\mathbf{k} = (0, 0)$. Also shown are the imaginary part of the self-energy and the crossing of the curves $\omega - \Omega_{\mathbf{k}}$ and $\text{Re } \Sigma(\mathbf{k}, \omega)$. The spectral functions are broadened by a small imaginary part $\eta = 0.005$ in ω .

FIG. 4. Polaron spectral density and self-energy for: a) $\mathbf{k} = (\pi/2, \pi/2)$ and b) $\mathbf{k} = 7(\pi/20, \pi/20)$ to distinguish a quasiparticle with infinite lifetime (a) and a finite one (b).

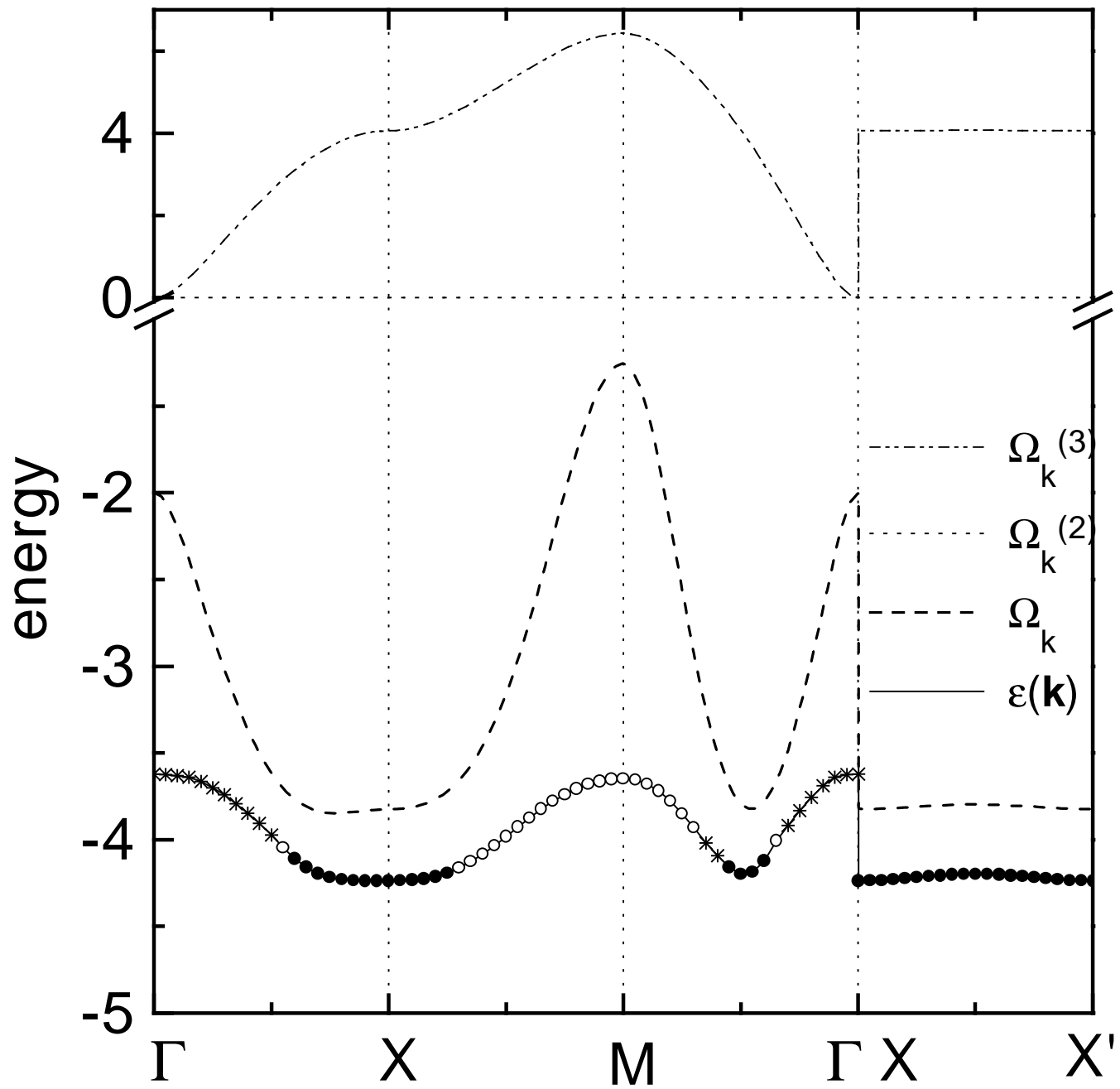
FIG. 5. Crossing of the curves $\varepsilon(\mathbf{q}')$ and $\varepsilon(\mathbf{k}) - \omega_{\mathbf{k}-\mathbf{q}'}$ for three different values of \mathbf{k} along the diagonal of the BZ for $\mathbf{q}' = (q'_x, q'_x)$: there are only trivial crossing points ($\mathbf{q} = \mathbf{k} - \mathbf{q}'$ equal to Γ or M) for $\mathbf{k} = (\pi/2, \pi/2)$ but nontrivial crossings for $\mathbf{k} = (4\pi/20, 4\pi/20)$ and $\mathbf{k} = (0, 0)$.

FIG. 6. Contour plot of hole spectral function $A_h(\mathbf{k}, \omega)$ for $J = 0.2$, $\tau = 1$, $h = 0.3$ and $\eta = 0.01$ along high symmetry lines in the BZ a) $(0, 0)$ - (π, π) , b) $(\pi, 0)$ - $(0, \pi)$ and c) $(0, 0)$ - $(\pi, 0)$.

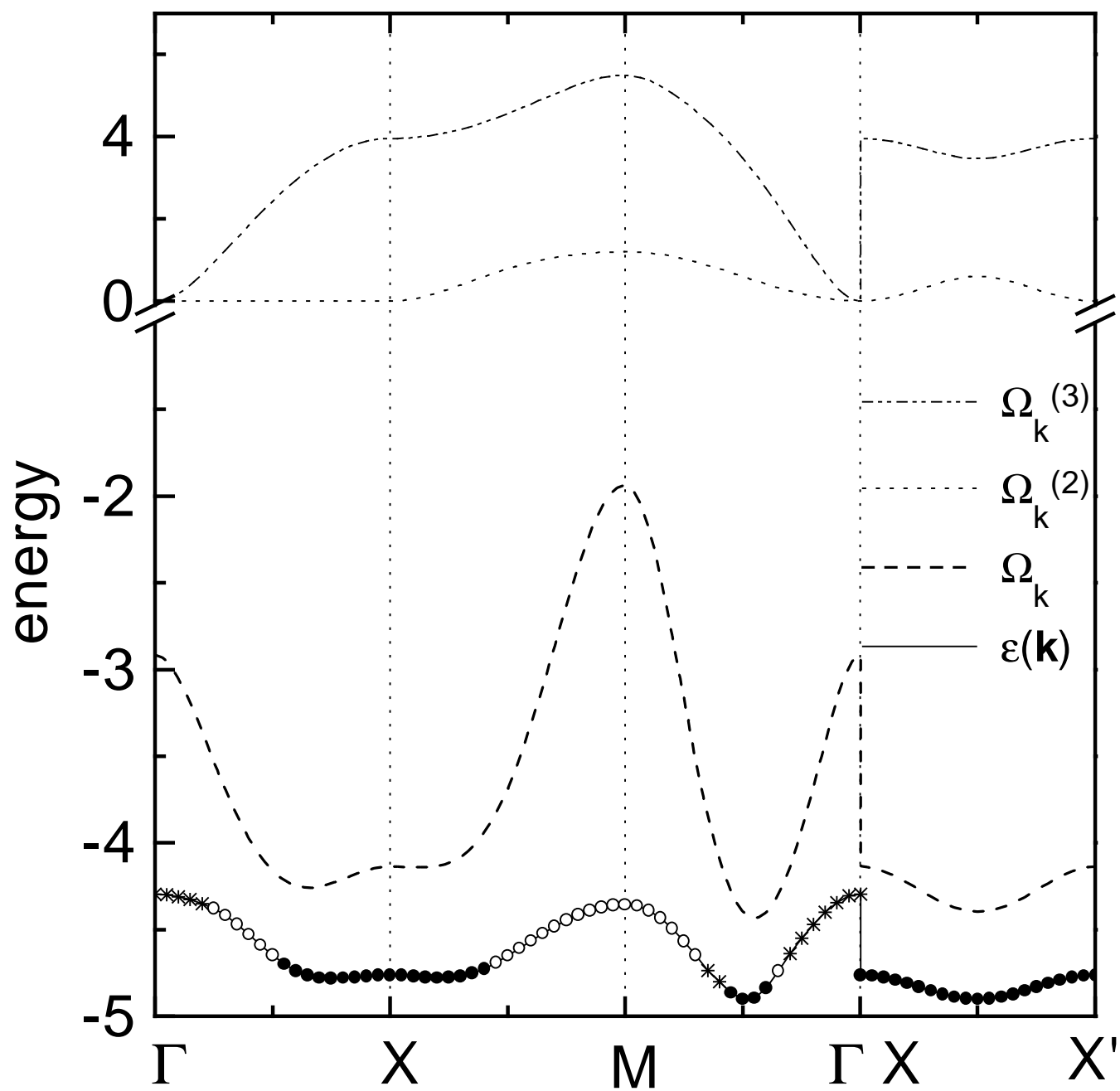
TABLE I. Position of the lowest energy peak $\varepsilon(\mathbf{k})$, the areas under the peak $W_p(\mathbf{k})$ and $W_h(\mathbf{k})$ and the imaginary part of the self-energy for $J/\tau = 0.2$, $h/\tau = 0.3$ and $\mathbf{k} = n(\pi/20, \pi/20)$

n	$\varepsilon(\mathbf{k})$	$W_p(\mathbf{k})$	$W_h(\mathbf{k})$	$-Im\Sigma(\mathbf{k}, \varepsilon(\mathbf{k}))$
0*	-4.30	0.020	0	0.1647
1*	-4.31	0.018	0.000	0.1751
2*	-4.35	0.008	0.001	0.1136
3*	-4.40	0.008	0.001	0.0999
4*	-4.47	0.010	0.002	0.0798
5*	-4.55	0.022	0.004	0.0472
6*	-4.64	0.061	0.013	0.0259
7◦	-4.74	0.718	0.170	0.0020
8●	-4.84	0.849	0.210	0.0000
9●	-4.89	0.850	0.218	0.0000
10●	-4.90	0.878	0.231	0.0000
11●	-4.86	0.785	0.212	0.0000
12*	-4.80	0.232	0.064	0.0148
13*	-4.74	0.059	0.017	0.0445
14◦	-4.65	0.100	0.029	0.0251
15◦	-4.57	0.095	0.029	0.0265
16◦	-4.50	0.116	0.037	0.0086
17◦	-4.43	0.132	0.044	0.0044
18◦	-4.39	0.145	0.051	0.0012
19◦	-4.36	0.148	0.053	0.0003
20◦	-4.36	0.146	0.053	0.0001

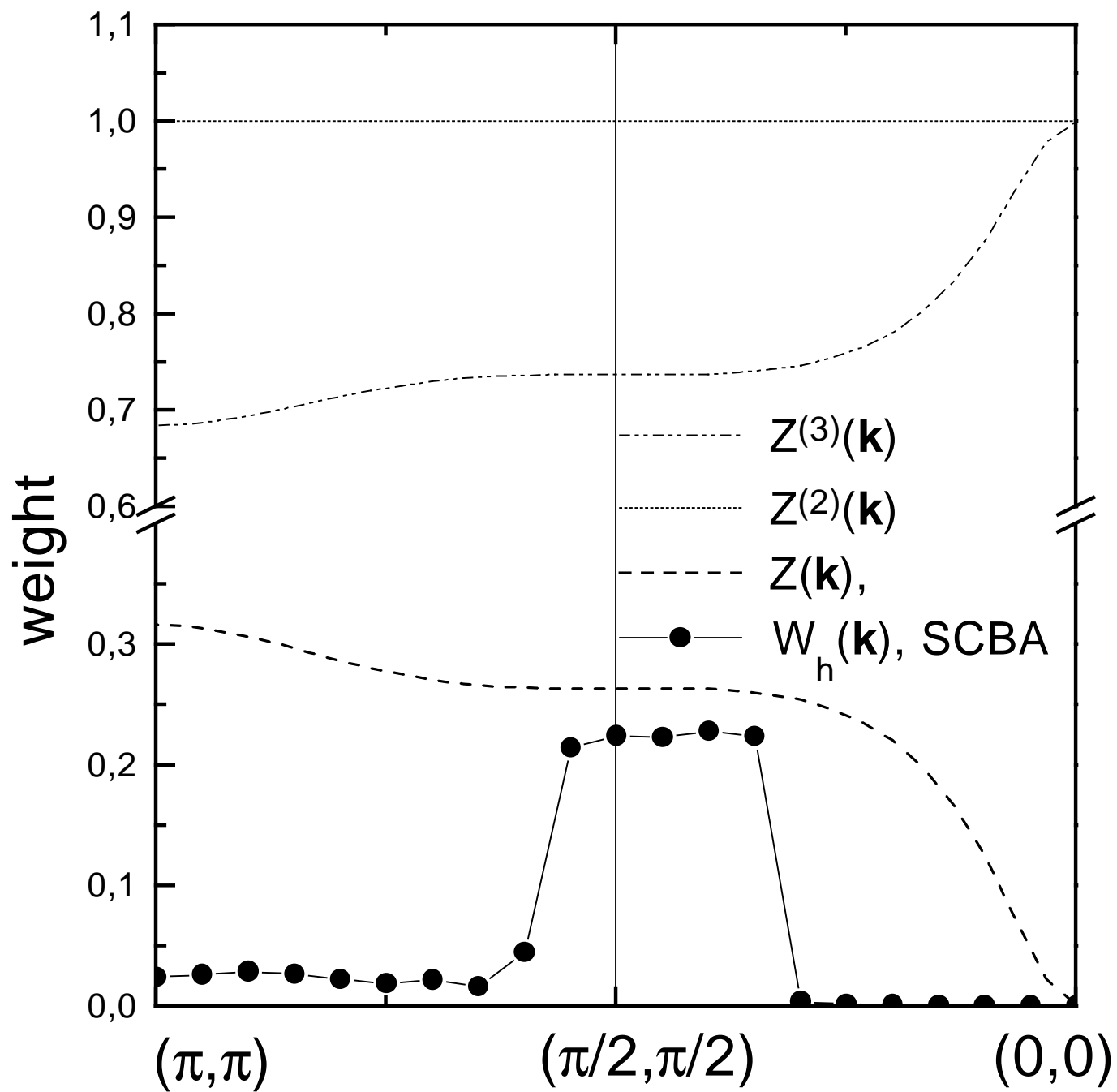
$\tau=1$ $J=0.2$ $h=0$



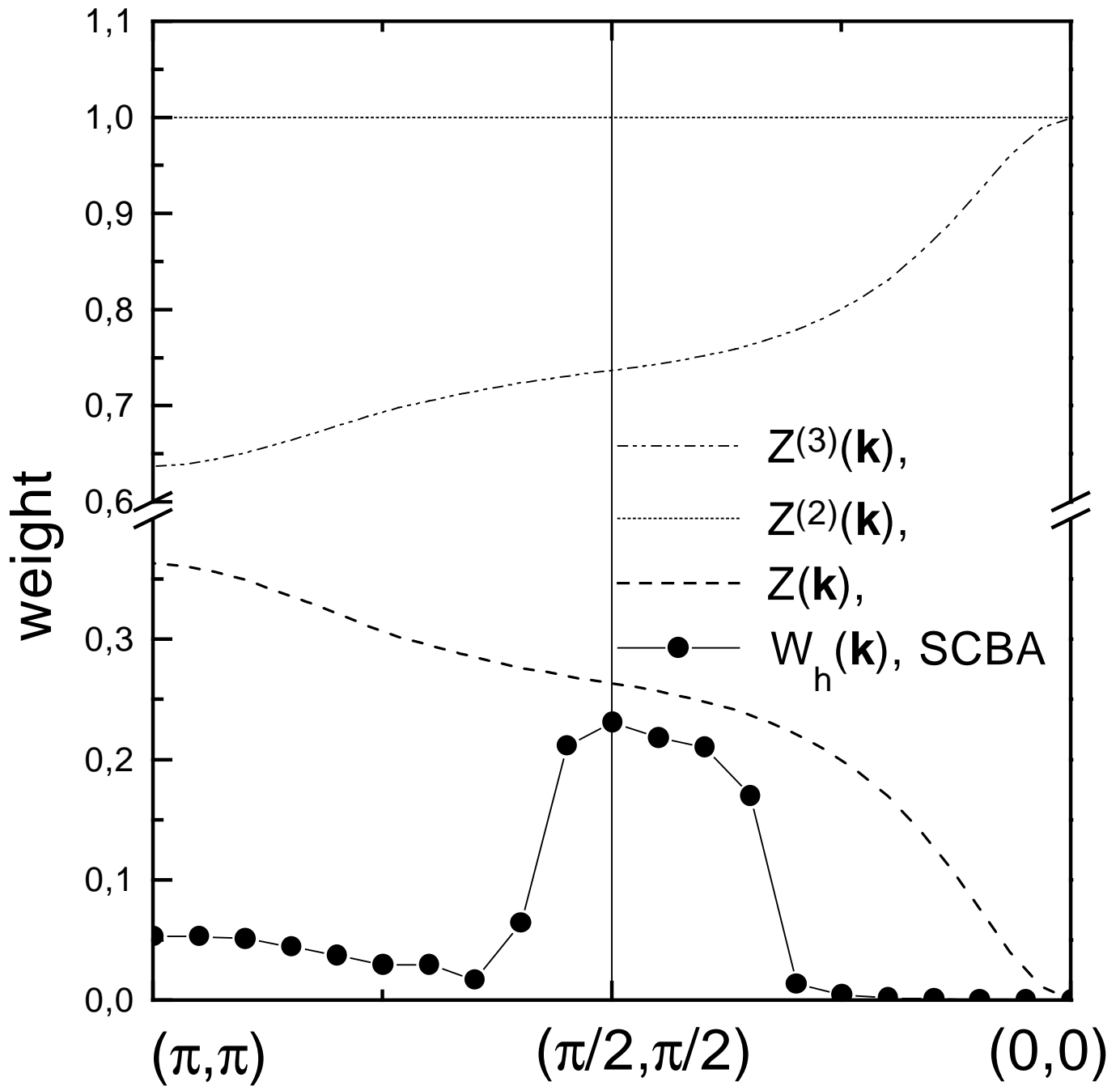
$\tau=1$ $J=0.2$ $h=0.3$



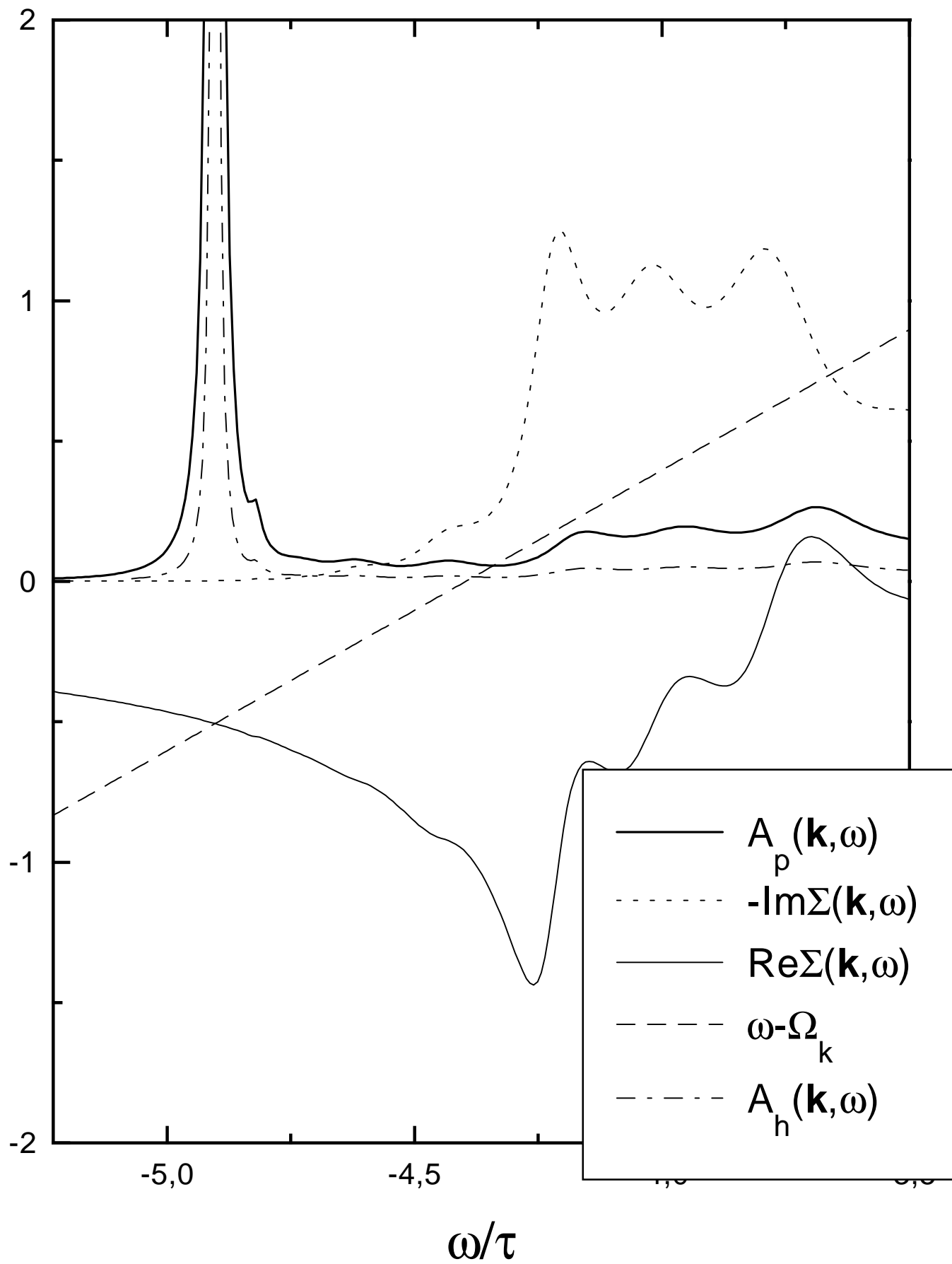
$\tau=1$ $J=0.2$ $h=0$



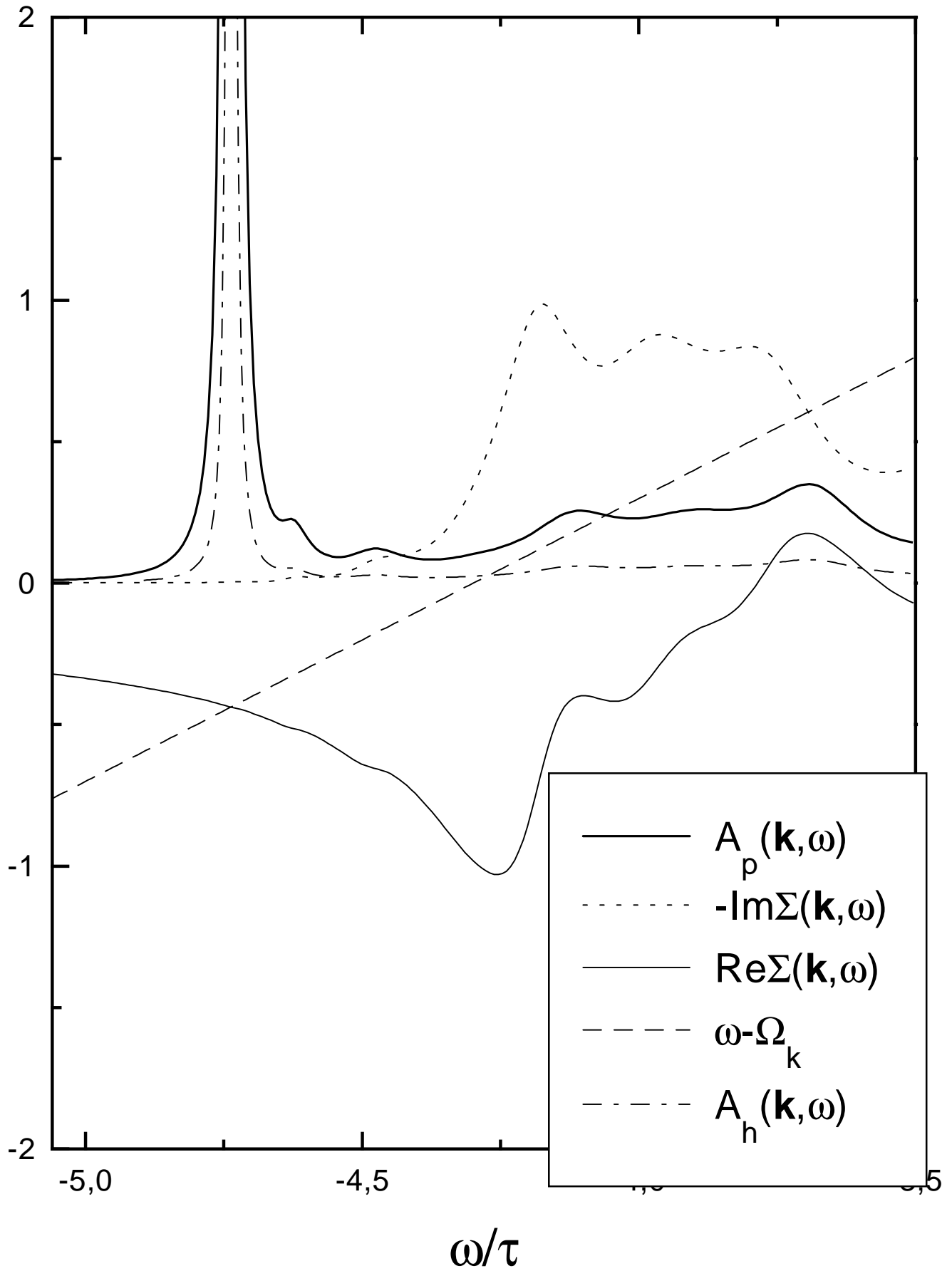
$\tau=1$ $J=0.2$ $h=0.3$



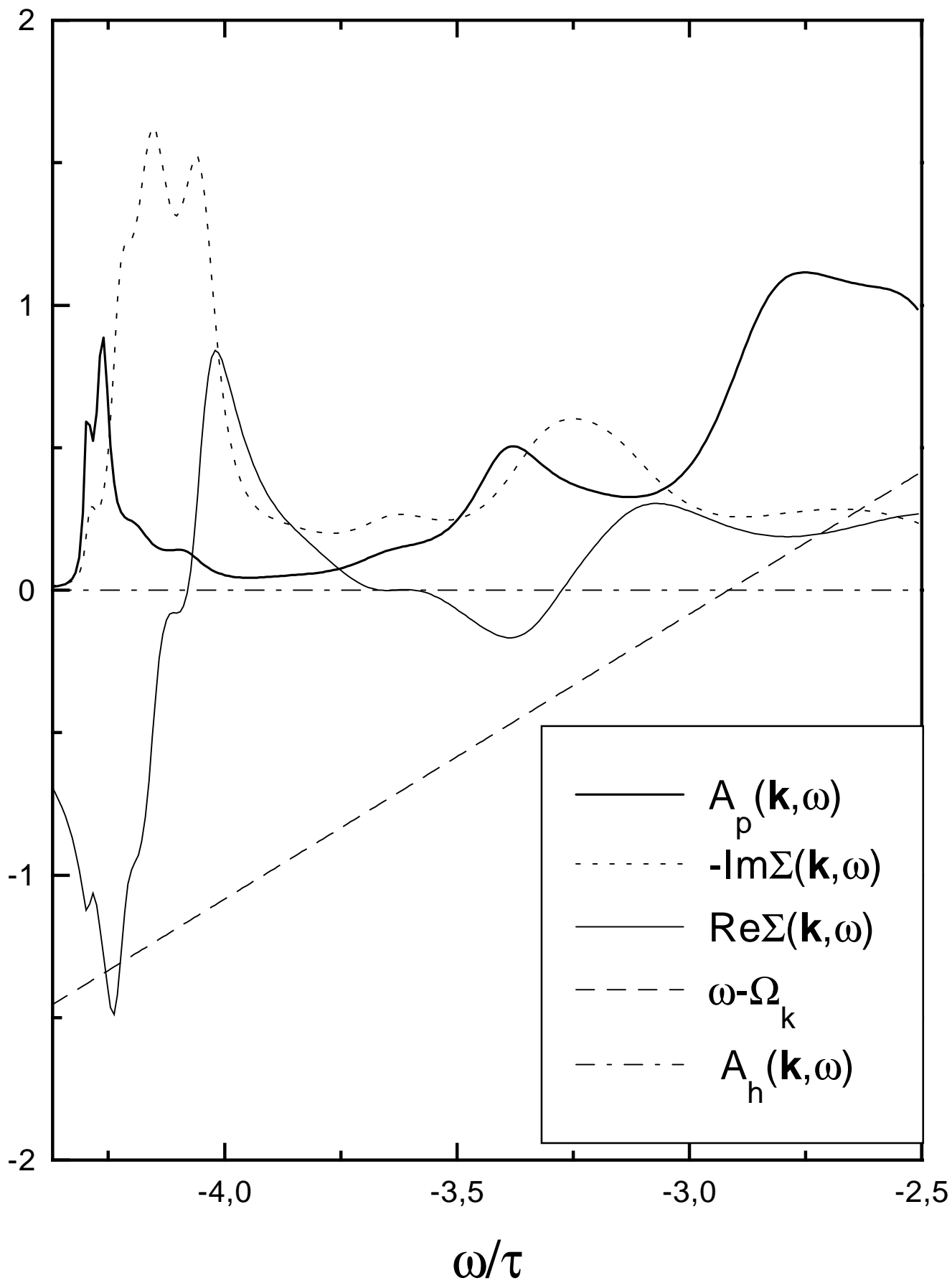
$\mathbf{k}=(\pi/2,\pi/2)$ $\tau=1$ $J=0.2$ $h=0.3$ $\eta=0.005$



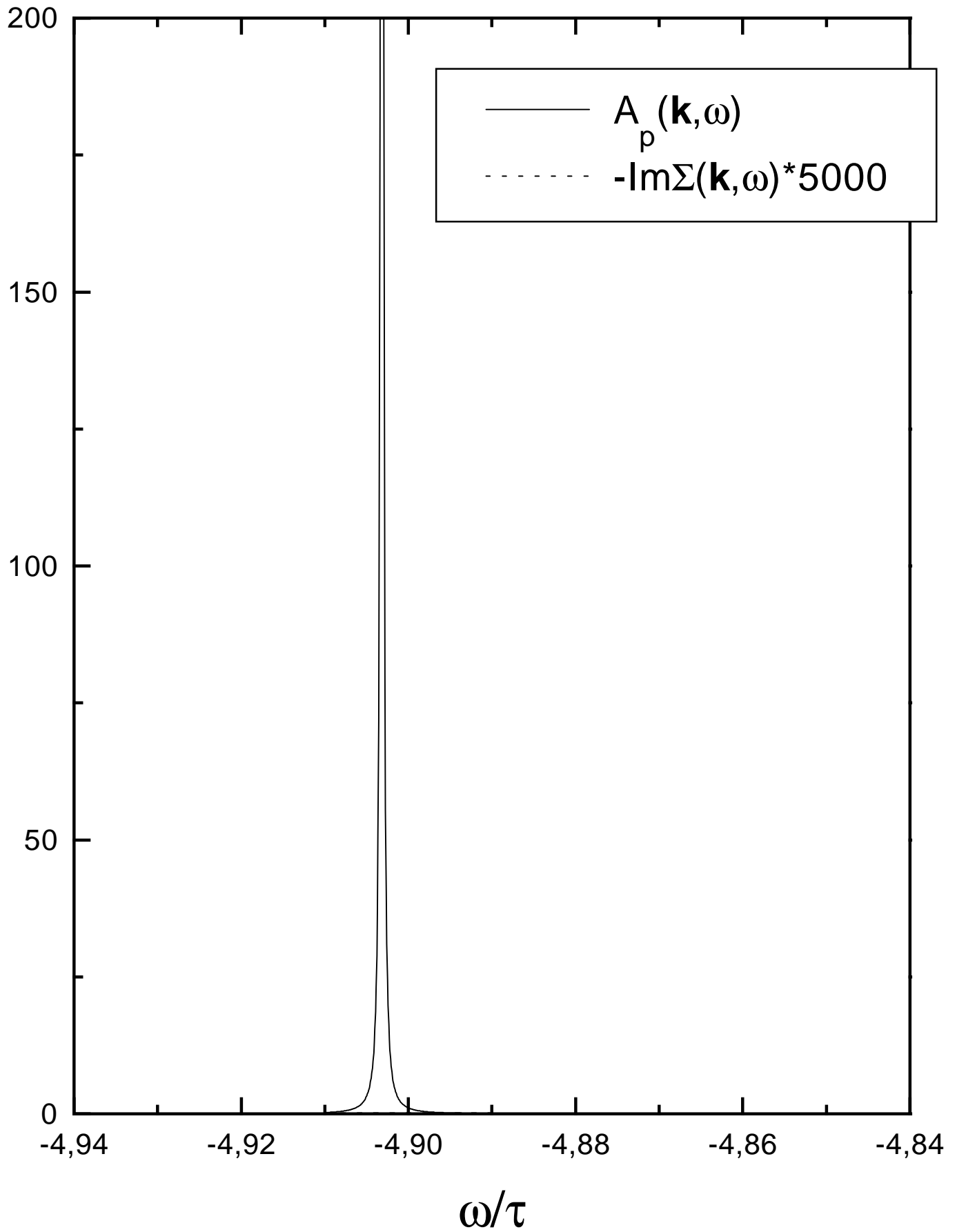
$\mathbf{k}=7^*(\pi/20,\pi/20)$ $\tau=1$ $J=0.2$ $h=0.3$ $\eta=0.005$



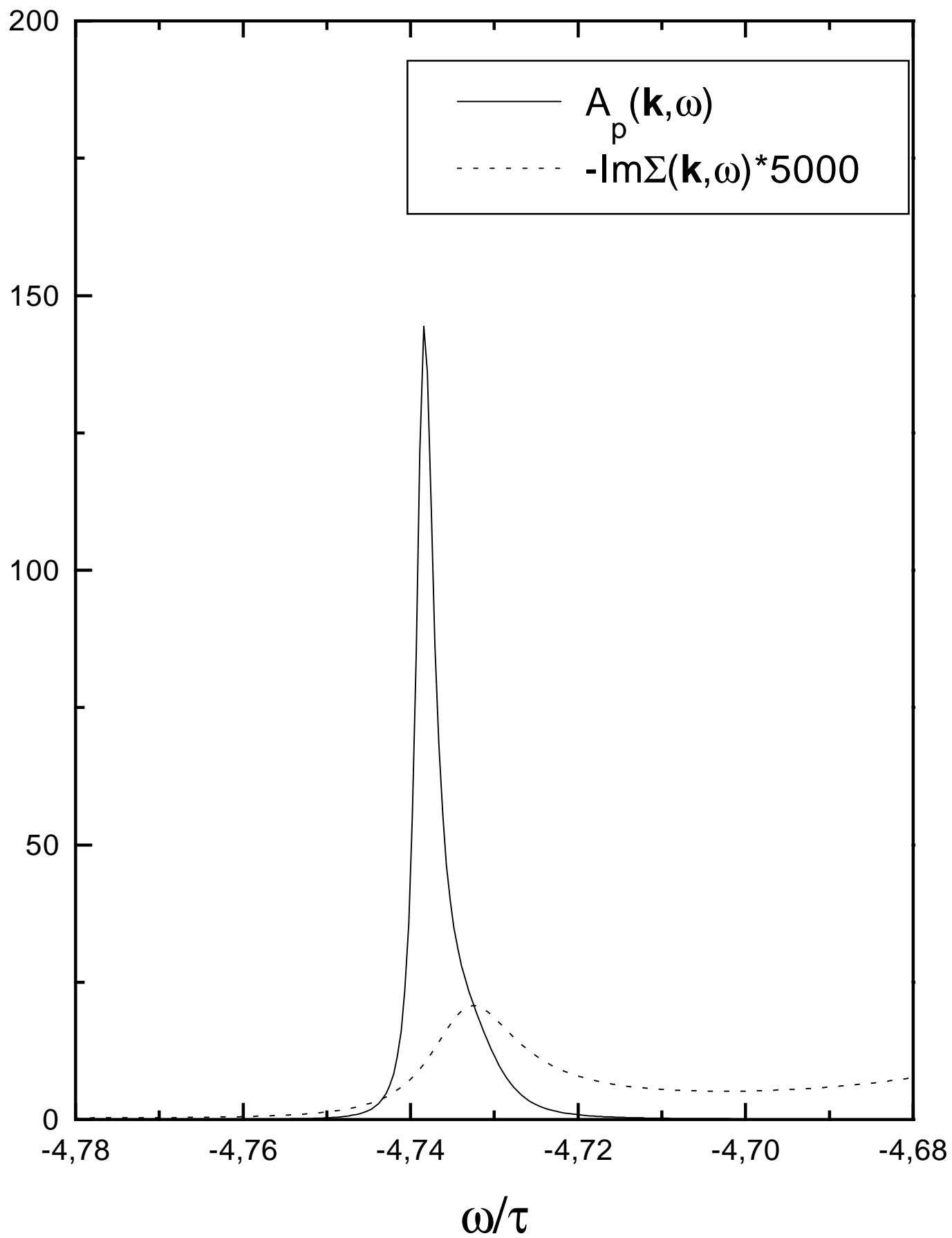
$\mathbf{k}=(0,0)$ $\tau=1$ $J=0.2$ $h=0.3$ $\eta=0.005$



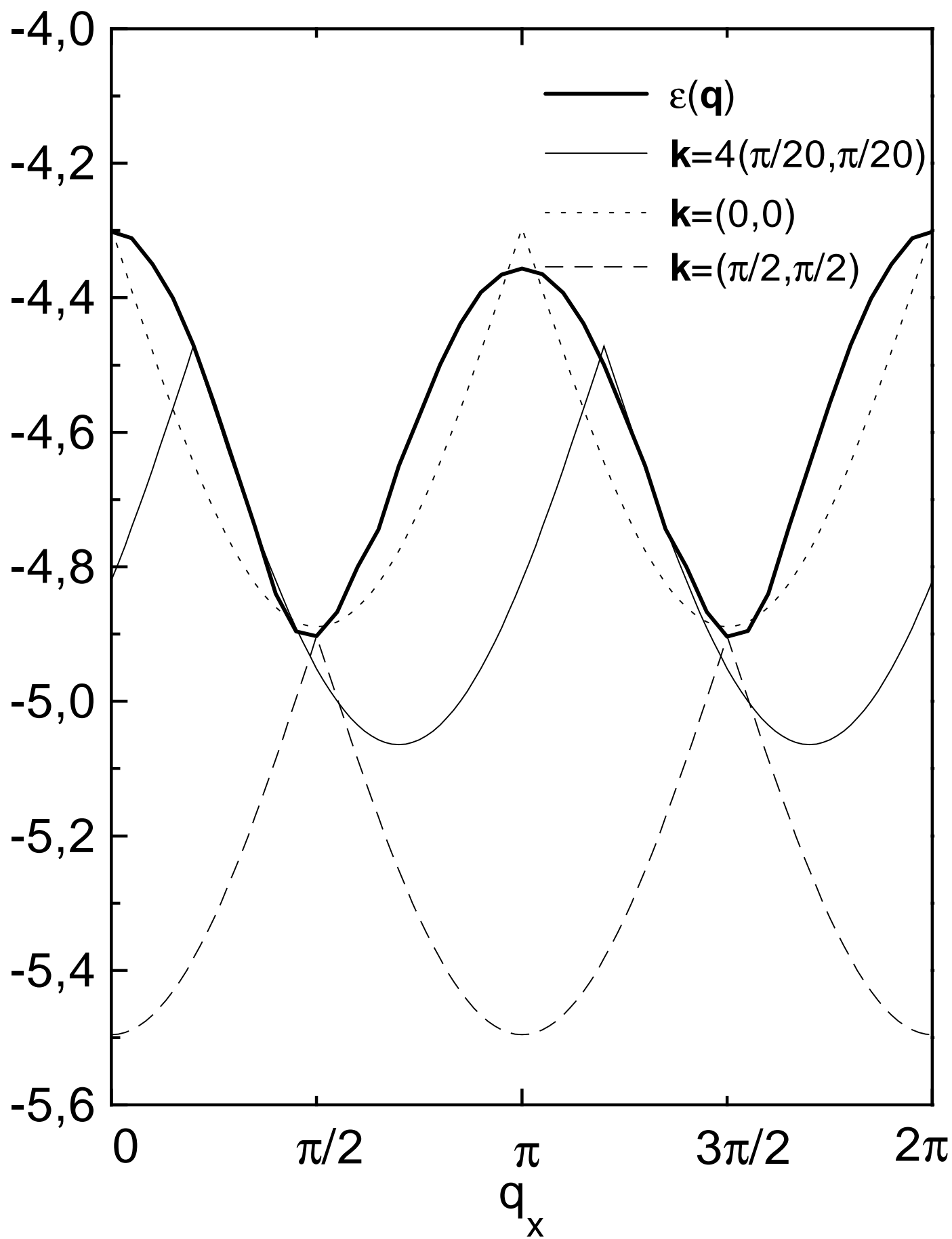
$\mathbf{k}=(\pi/2,\pi/2)$ $\tau=1$ $J=0.2$ $h=0.3$ $\eta=0.00005$



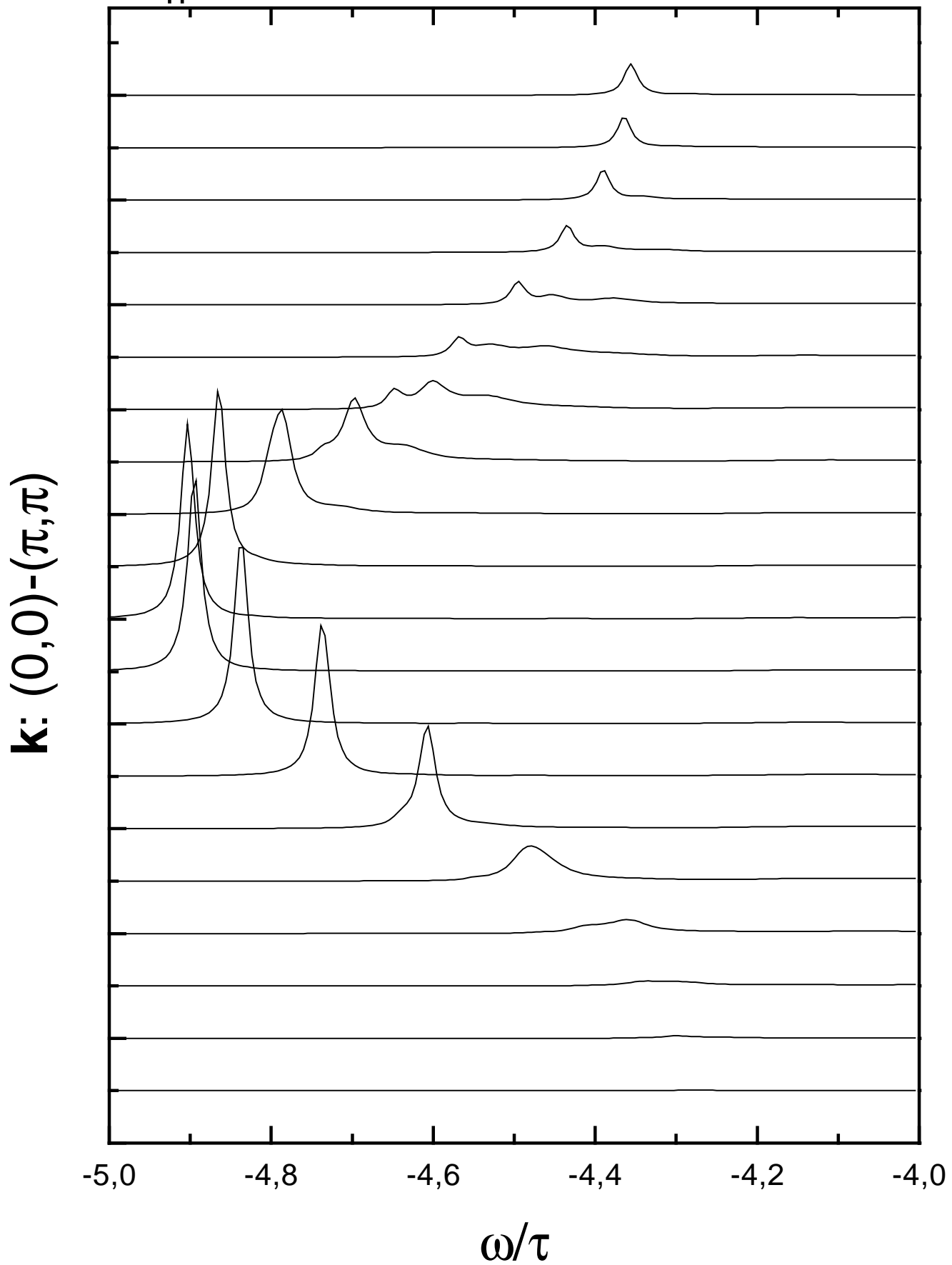
$\mathbf{k}=7^*(\pi/20,\pi/20)$ $\tau=1$ $J=0.2$ $h=0.3$ $\eta=0.00005$



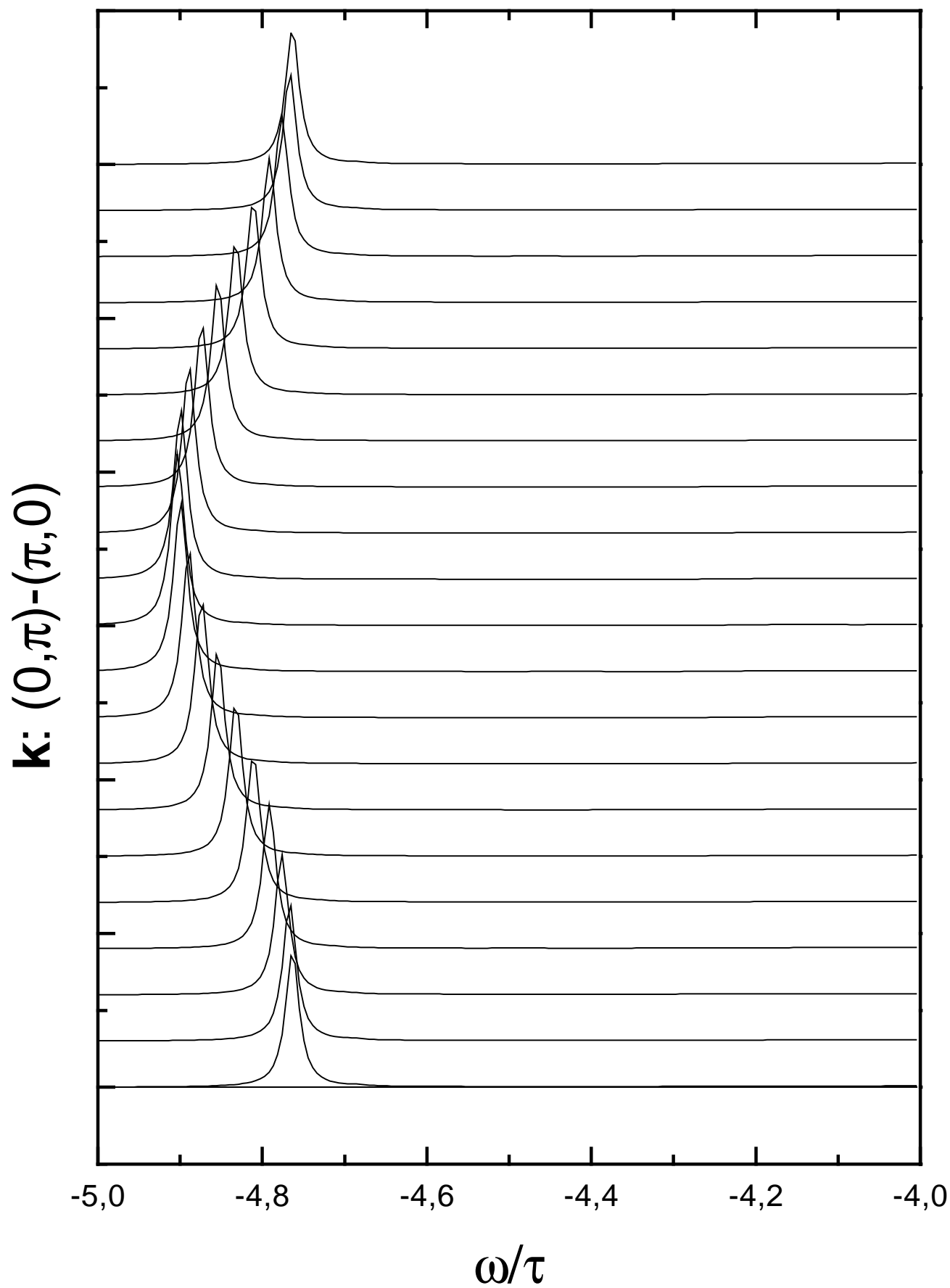
$\tau=1$ $J=0.2$ $h=0.3$



$A_h(\mathbf{k}, \omega)$ $\tau=1$ $J=0.2$ $h=0.3$ $\eta=0.01$



$A_h(\mathbf{k}, \omega)$ $\tau=1$ $J=0.2$ $h=0.3$ $\eta=0.01$



$A_h(\mathbf{k}, \omega), \tau=1 \quad J=0.2 \quad h=0.3 \quad \eta=0.01$

